Chapter 5

Hierarchical Scheduling of Active Distribution System with Multi-Microgrid

5.1 Introduction

Multiple autonomous microgrids connected to an Active Distribution Network (ADN) improves the flexibility and reliability of the supply system. Microgrids (MGs) are entities with multiple resources, such as Renewable Energy Sources (RESs), dispatchable Distributed Generations (DGs), Battery Energy Storage System (BESS), and consumers participating in Demand Response (DR). MG plays an important role in energy management system due to its wide variability and flexibility in generation and consumption. Traditionally, the Microgrid Operator (MGO) is responsible for MG's Energy Management System (EMS) to achieve objectives, such as reducing the cost of distributed energy resources and energy purchase from the Distribution Utility (DU), and incorporating demand response mechanisms for flexible loads. In the present scenario, a microgrid may consist of multiple decision-making entities with rationality and autonomy, which can have different objectives of power exchange. Therefore, EMS aimed only at reducing the operating cost of MGO may not be suitable for the modern electricity trading scenario. Also, the interconnection of multiple microgrids in the distribution system provides an opportunity for internal competitive power trading.

The previous chapter addresses the energy management of Multi-Microgrid (MMG)

system. This chapter incorporates the role of DU in the energy management of ADN with MMG. The power trading model considering operating agents at different levels such as DU, MGOs, and end-users lends opportunity for the coordination and effective utilization of energy resources. The decisions of all the agents are interlinked and can be realized using a hierarchical Stackelberg game model. For example, the power procurement of a DU from the main grid, and the technical considerations of the distribution network depend on the power exchange request of MGs. Further, the dispatch strategies of MGs depend on their power generation as well as demand profile of their end-users. The techno-economic aspects can be accomplished more effectively if the energy management framework considers hierarchically coordinated decisions making of all the agents. This chapter proposes an energy management framework incorporating a three-level hierarchical decision approach, through which multiple operating agents can actively participate in the energy management to achieve their respective goals. In this framework, a game-theoretic dynamic pricing scheme is used to enable the interaction between the DU and MGOs as well as between the MGO and End-User Aggregators (EUAs) to take advantage of the follower's flexibility to improve the technical and economic aspects. Also, this arrangement enables end-user aggregators to negotiate adequately with microgrid operators.

The Info-Gap Decision Theory (IGDT) based model captures the uncertainties associated with RESs. The impact of risk-averse and risk-seeker decisions of MGOs on the operating cost of DU is also investigated in this chapter. The above-mentioned contributions of this chapter can be summarized as follows.

- An energy management framework is developed with hierarchical decision making of DU, MGOs and EUAs through which all the players can actively participate in the energy management to achieve their respective goals.

- A game-theoretic dynamic pricing scheme is used for the interaction between DU and MGOs as well as between MGO and EUAs to take advantage of the follower's flexibility to improve the technical and economic aspects.

- A Info-Gap Decision Theory (IGDT) based model capturing RESs uncertainties has been applied to assess the effect of risk-averse and risk-seeking decision making of MGOs on DU benefits.

5.2 System model

This work presents an interactive energy management for an active distribution system with multi-microgrids connected to the network, considering the hierarchical decision making of different players at each level. The conceptual scheme of three-level hierarchical decision making is shown in the Figure 5.1. The distribution system is connected to the main grid at the PCC. The DU manages its dispatchable DGs, power exchange with the main grid, power exchange with the MGOs, and consumer load connected at different buses. In this work, it is assumed that each MG may consist of EVs, BESSs, DR loads, dispatchable DG and RESs (i.e., Wind-Turbine (WT) and Photovoltaic (PV)). To emphasize the active participation of end-users as stakeholders, each MG is divided into several groups of DR loads, BESSs, and EVs, i.e. End-User Aggregators (EUAs). The EUAs are responsible for managing the shiftable load of their consumers based on tariffs provided by the MGO. DU and MGO are inter-dependent in their decision making, that is, the decisions of the DU influence the decisions of the MGOs and vice-versa. Similarly, the decisions of the MGO and the EUA are also interlinked. The MGOs are intermediary between DU and EUAs. The MGO acts as a follower of the DU and leader of the EUAs.

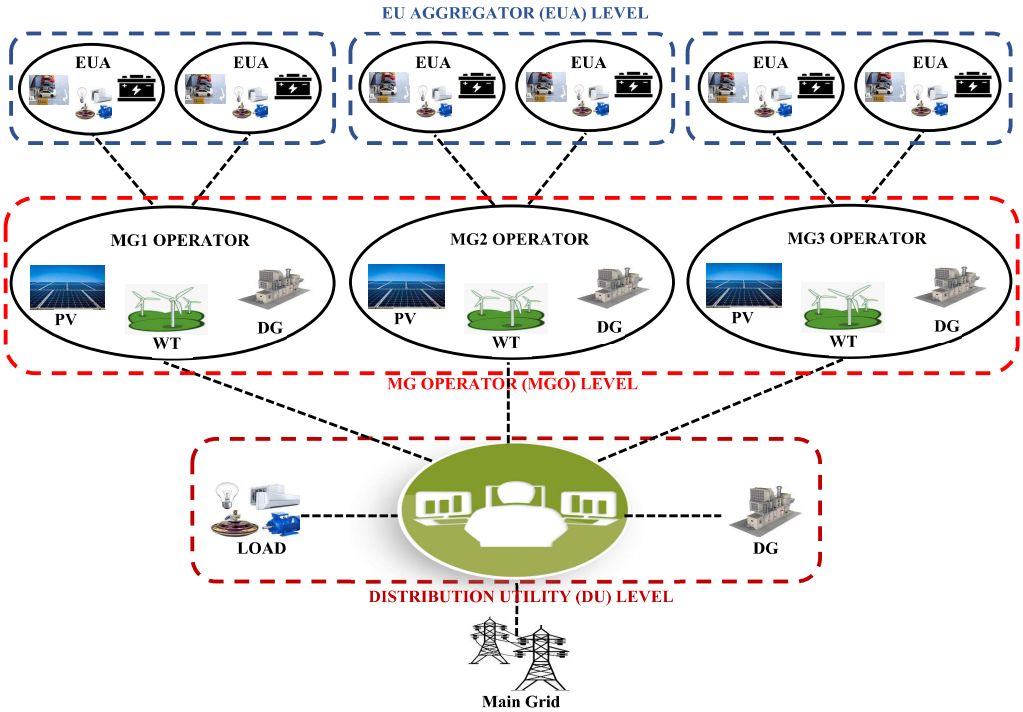

Figure 5.1: Conceptual scheme of hierarchical three-level energy management

The detailed mechanism of this energy management framework is described in section 5.4.

5.3 Problem formulation for different decision making agents

5.3.1 End-User Aggregator (EUA) level modeling

In each MG premise, the EUAs are load-serving entities for Demand-Responsive (DR) loads and charging stations. The EUAs aim to maximize their profits based on the tariff offered by MGO. The profit of n^{th} EUA under m^{th} MG, can be defined as,

$$F_{EUA}^{n} = \sum_{t=1}^{T} \left(\sum_{n_B=1}^{N_B} d_t^{n_B,n} \rho_t^{n_B,n} - P_t^n \rho_t^m - \left(P_t^{d,b,n} + \sum_{ev=1}^{N_{ev}} P_t^{d,ev,n} \right) \rho^d \right). \tag{5.1}$$

The first term is the gain derived from the energy delivered to the DR loads. The second term represents the cost of power exchange with MGO. Degradation of batteries in BESS and PHEVs is minimized by adding a penalty term for battery discharging. The tariff of MGO to EUA, ρ_t^m is the MGO level variable, and this is considered as a parameter at EUA level.

The DR is modeled by the Time-of-Use (TOU) price and step-wise decreasing price curve [133]. As shown in Figure 5.2, the demand-responsive load price decreases as demand increases. The horizontal dotted line depicts the power purchase price of EUA at t^{th} hour. The EUA profit to meet the demand increases up to point B; after point B profits begin to decline. Thus, EUA adjusts the load according to the price curve and the power purchase price for a time interval. The DR load is subjected to the following

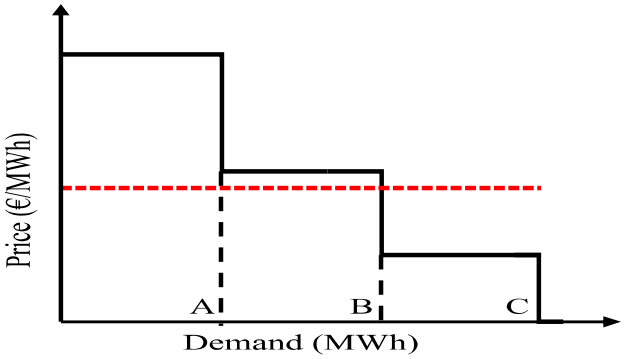

Figure 5.2: Step-wise price curve for DR load

constraints.

$$0.9P_t^{0,n} \leq P_t^{DR,n} \leq 1.1P_t^{0,n} \qquad : \mu_t^{1,n}, \mu_t^{2,n} \tag{5.2}$$

$$\sum_{t=1}^{T} \left(P_t^{0,n} - P_t^{DR,n} \right) \leq \zeta \sum_{t=1}^{T} P_t^{0,n} \qquad : \mu^{3,n} \tag{5.3}$$

$$P_t^{DR,n} = \sum_{n_B=1}^{N_B} d_t^{n_B,n} \qquad : \lambda_t^{1,n} \tag{5.4}$$

$$0 \leq d_t^{n_B,n} \leq d^{max,n_B,n} \qquad : \mu_t^{4,n_B,n}, \mu_t^{5,n_B,n} \tag{5.5}$$

Equation (5.2) limits the load shifting in DR. The maximum allowable load curtailment is constrained by Equation (5.3). Equations (5.4) and (5.5) are used to obtain the optimal power from each step to satisfy the scheduled DR load.

The BESS and PHEV models can be described by using the following constraints.

$$E_t^{b,n} = \eta_{sd} E_{t-1}^{b,n} + \eta_c P_t^{c,b,n} - \frac{P_t^{d,b,n}}{\eta_d} \qquad : \lambda_t^{2,n} \tag{5.6}$$

$$0 \leq P_t^{c,b,n} \leq P^{cmax,b,n} \qquad : \mu_t^{6,n}, \mu_t^{7,n} \tag{5.7}$$

$$0 \leq P_t^{d,b,n} \leq P^{dmax,b,n} \qquad : \mu_t^{8,n}, \mu_t^{9,n} \tag{5.8}$$

$$E^{min,b,n} \leq E_t^{b,n} \leq E^{max,b,n} \qquad : \mu_t^{10,n}, \mu_t^{11,n} \tag{5.9}$$

$$\sum_{t=1}^{T} \left(\eta_c P_t^{c,b,n} - \frac{P_t^{d,b,n}}{\eta_d} - (1 - \eta_{sd}) E_{t-1}^{b,n} \right) = 0 \qquad : \lambda^{3,n} \tag{5.10}$$

$$E_t^{ev,n} = \eta_{sd} E_{t-1}^{ev,n} + \eta_c P_t^{c,ev,n} - \frac{P_t^{d,ev,n}}{\eta_d} \qquad : \lambda_t^{4,ev,n} \qquad \forall t \in (t_{arri}, t_{depa}) \tag{5.11}$$

$$0 \leq P_t^{c,ev,n} \leq P^{cmax,ev,n} \qquad : \mu_t^{12,ev,n}, \mu_t^{13,ev,n} \qquad \forall t \in (t_{arri}, t_{depa}) \tag{5.12}$$

$$0 \leq P_t^{d,ev,n} \leq P^{dmax,ev,n} \qquad : \mu_t^{14,ev,n}, \mu_t^{15,ev,n} \qquad \forall t \in (t_{arri}, t_{depa}) \tag{5.13}$$

$$E^{min,ev,n} \leq E_t^{ev,n} \leq E^{max,ev,n} \qquad : \mu_t^{16,ev,n}, \mu_t^{17,ev,n} \qquad \forall t \in (t_{arri}, t_{depa}) \tag{5.14}$$

$$E_t^{ev,n} = E_{t_{depa}}^{ev,n} \qquad : \lambda_{t_{depa}}^{5,ev,n}, \qquad \forall t \in t_{depa} \tag{5.15}$$

$$E_t^{ev,n} = E_{t_{arri}}^{ev,n} + \eta_c P_t^{c,ev,n} - \frac{P_t^{d,ev,n}}{\eta_d} \qquad : \lambda_{t_{arri}}^{6,ev,n}, \forall t \in t_{arri} \tag{5.16}$$

$$-P^{evmax} \leq \sum_{ev=1}^{N_{ev}} (P_t^{c,ev,n} - P_t^{d,ev,n}) \leq P^{evmax} \qquad : \mu_t^{18,n}, \mu_t^{19,n} \tag{5.17}$$

The next stage energy level of battery depends on the present energy level and charging/discharging power status, and this relation for BESS and PHEVs can be defined by Equations (5.6) and (5.11), respectively. The maximum charging and discharging powers

of BESSs and PHEVs are constrained by Equations (5.7), (5.8), (5.12), and (5.13). The battery energy levels are subjected to maximum and minimum limits, and these limits are imposed by Equations (5.9) and (5.14) for BESSs and PHEVs, respectively. The Equation (5.10) ensures that the net power exchange from BESSs equals zero. The PHEVs energy level at departure and arrival must satisfy the constraints (5.15) and (5.16). The total power demand of all PHEVs under an EUA is restricted by the constraint (5.17).

The following constraints represent the load balance and power exchange limit of EUA with MGO.

$$P_t^n - P_t^{DR,n} - P_t^{c,b,n} + P_t^{d,b,n} - \sum_{ev=1}^{N_{ev}} (P_t^{c,ev,n} - P_t^{d,ev,n}) = 0 \qquad : \lambda_t^{7,n} \tag{5.18}$$

$$-P^{max,n} \leq P_t^n \leq P^{max,n} \qquad : \mu_t^{20,n}, \mu_t^{21,n} \tag{5.19}$$

5.3.2 Microgrid operator level modeling

The MGO interacts with EUAs to decide optimal tariff according to the power exchange request received from all EUAs. The power exchange price offered by DU depends on the strategies of all MGOs as well as the DU. Thus, the MGO maximizes its profits, F_{MGO}^m, based on the tariff proposed by the DU and power exchange request received from EUAs. The MGO's objective function consists of income from EUAs, power exchange cost from DU, dispatchable DG generation cost, and emission cost due to power generation from dispatchable DG. The profit of m^{th} MGO can be defined as

$$F_{MGO}^m = \sum_{t=1}^{T} \left(\sum_{n=1}^{N_{EUA}} P_t^n \rho_t^m - P_t^m \rho_t^{du} - \rho^{dg,m} P_t^{dg,m} - \rho^{emi} P_t^{dg,m} \right). \tag{5.20}$$

Here, ρ_t^{du} is the power exchange price for MGO. This price can be described as follows.

$$\rho_t^{du} = \rho_t^{base} + \delta\big(P_t^m + \sum_{-m} P_t^{-m} + P_t^{L,du}\big). \tag{5.21}$$

P_t^{-m} is the power exchange request received from MGOs except the m^{th} MGO and $P_t^{L,du}$ is the load demand of consumers of DU. These two terms are considered as parameters for m^{th} MGO. The base price, ρ_t^{base} is the DU level variable, and this is considered as a parameter for MGO. The coefficient, δ, is a predetermined DU parameter. Therefore, the objective function (5.20) is quadratic in nature. The constraints for the MGO objective are as follows.

$$-P^{max,m} \leq P_t^m \leq P^{max,m} \qquad : \mu_t^{22,m}, \mu_t^{23,m} \tag{5.22}$$

$$\rho^{min,m} \leq \rho_t^m \leq \rho^{max,m} \qquad : \mu_t^{24,m}, \mu_t^{25,m} \tag{5.23}$$

$$\sum_{t=1}^{T} \rho_t^m \leq \rho^{avg,m} T \qquad : \mu^{26,m} \tag{5.24}$$

$$0 \leq P_t^{dg,m} \leq P^{DGmax,m} \qquad : \mu_t^{27,m}, \mu_t^{28,m} \tag{5.25}$$

$$P_t^m - \sum_{n=1}^{N_{EUA}} P_t^n + P_t^{dg,m} + P_t^{RES,m} = 0 \qquad : \lambda_t^{8,m} \tag{5.26}$$

$$P_{t-1}^{dg,m} - P_t^{dg,m} \leq RD^{dg,m} \qquad : \mu_t^{29,m} \tag{5.27}$$

$$P_t^{dg,m} - P_{t-1}^{dg,m} \leq RU^{dg,m} \qquad : \mu_t^{30,m} \tag{5.28}$$

The Equation (5.22) imposes the maximum limits for power import (export) from (to) the distribution network. The Equation (5.23) restricts the power exchange price offered by MGO to EUAs, between upper and lower caps. Also, the average price should be less than the specified limit as depicted by Equation (5.24). Dispatchable DG power limits are represented by Equation (5.25). The load balancing constraint is given in Equation (5.26). The constraints in Equations (5.27) and (5.28) describe ramp-down and ramp-up limits of dispatchable DGs, respectively. The uncertainties related to RESs are handled with IGDT. The detailed description of IGDT is given in section 5.4.

5.3.3 Distribution utility level modeling

The DU aims to minimize its operating cost as well as voltage deviation such that all the network conditions must satisfy. The objective functions of DU to be minimized can be written as follows.

$$F_{DU}^C = \sum_{t=1}^{T} \Bigg(P_t^g \rho_t^g + \sum_{dg=1}^{N_{dg}} (\rho^{dg,du} P_t^{dg,du} + \rho^{emi} P_t^{dg,du}) - \sum_{k=1}^{N_{bus}} P_t^{L,k} \rho_t^{du} + \sum_{k} P_t^{loss,sop,k} \rho_t^g \Bigg). \tag{5.29}$$

The cost related objective (5.29) has main grid power exchange cost, dispatchable DG generation cost, emission cost due to power generation from DG, income from consumer load, and cost of power loss in Soft Open Point (SOP).

$$F_{DU}^V = \sum_{t=1}^{T} \sum_{k=1}^{N_{bus}} V_t^{dev,k}. \tag{5.30}$$

The second objective (5.30) is used to minimize the voltage deviation of all buses from nominal value. The term $V_t^{dev,k}$ can be defined as

$$V_t^{dev,k} = |V^{rated} - V_t^k|. \tag{5.31}$$

The DU has following distribution network related constraints.

$$\rho^{min,base} \leq \rho_t^{base} \leq \rho^{max,base}, \tag{5.32}$$

$$\sum_{t=1}^{T} \rho_t^{base} \leq \rho^{avg,base} T, \tag{5.33}$$

$$-P^{max,du} \leq P_t^g \leq P^{max,du}, \tag{5.34}$$

$$(P_t^{k,j})^2 + (Q_t^{k,j})^2 \leq (S^{max,k,j})^2, \tag{5.35}$$

$$V^{min} \leq V_t^k \leq V^{max}, \tag{5.36}$$

$$\sum_j P_t^{k,j} - x_{PCC}^k P_t^g - \sum_{dg=1}^{N_{dg}} x_{dg}^k P_t^{dg,du} + P_t^{L,k} + \sum_{m=1}^{N_{MG}} x_m^k P_t^m + \sum_{sop=1}^{N_{sop}} x_{sop}^k P_t^{sop,k} = 0, \tag{5.37}$$

$$\sum_j Q_t^{k,j} - x_{PCC}^k Q_t^g + Q_t^{L,k} + \sum_{sop=1}^{N_{sop}} x_{sop}^k Q_t^{sop,k} = 0, \tag{5.38}$$

$$-(1-\nu^{k,j})M \leq V_t^k - V_t^j - \frac{R^{k,j} P_t^{k,j} + X^{k,j} Q_t^{k,j}}{V^{rated}} \leq (1-\nu^{k,j})M, \tag{5.39}$$

$$-\nu^{k,j} P^{max,k,j} \leq P_t^{k,j} \leq \nu^{k,j} P^{max,k,j}, \tag{5.40}$$

$$-\nu^{k,j} Q^{max,k,j} \leq Q_t^{k,j} \leq \nu^{k,j} Q^{max,k,j}, \tag{5.41}$$

$$P_t^{sop,k} + P_t^{sop,j} + P_t^{loss,sop,k} + P_t^{loss,sop,j} = 0, \tag{5.42}$$

$$(P_t^{sop,k})^2 + (Q_t^{sop,k})^2 \leq (S^{sop,k})^2, \tag{5.43}$$

$$P_t^{loss,sop,k} = A^{sop,k} \sqrt{(P_t^{sop,k})^2 + (Q_t^{sop,k})^2}. \tag{5.44}$$

The base price offered by DU to MGOs is restricted by upper and lower limits, as shown in Equation (5.32). The Equation (5.33) implies that the average base price should be less than the specified limit. The constraints (5.34), (5.35), and (5.36) limit the DU power exchange with the main grid, line loading, and bus voltage magnitude, respectively. The linear DistFlow model [134] is used in this work. The Equations (5.37)-(5.41) are associated with linear power flow constraints. DU active power balance at each bus is

represented by constraint (5.37). The Equation (5.38) specifies the reactive power balance at each bus. The voltage relationship between the two buses is expressed in Equation (5.39). Here, a large integer, M, decouples the voltage levels of two disconnected buses. The steady-state model of SOP [135] can be described by Equations (5.42)-(5.44). The active power balance constraint of SOP is shown in Equation (5.42). The power loss of the voltage source converter in SOP can be calculated as described in Equation (5.44).

The feasible region of circular constraints (5.35) and (5.43) can be defined as the interior region of the circles of radius $S^{max,k,j}$ and $S^{sop,k}$, respectively. A circular region can be approximated by a polygon with H edges (ideally a polygon with ∞ edges), as shown in Figure 5.3. [136]

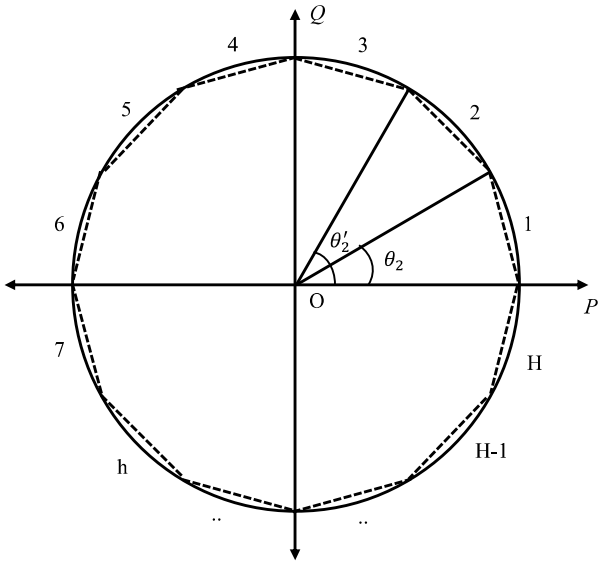

Figure 5.3: Circular constraints approximation

The circular constraint can be replaced by H linear constraints as follows.

$$P(sin\theta_h^{'} - sin\theta_h) + Q(cos\theta_h - cos\theta_h^{'}) + Ssin(\theta_h - \theta_h^{'}) \leq 0 \qquad h \in [1, H]. \quad (5.45)$$

Here, θ_h and $\theta_h^{'}$ associated with h^{th} edge can be written as,

$$\theta_h = \frac{2\pi(h-1)}{H},$$

and

$$\theta_h^{'} = \frac{2\pi h}{H}.$$

Similarly, the constraint (5.44) can be linearized by introducing an auxiliary variable $P_t^{aux,sop,k}$. The apparent power-bound parameter, S in the Equation (5.45) can be replaced by the variable $P_t^{aux,sop,k}$. The variable, $P_t^{aux,sop,k}$ represents the variable radius of a circle. It should be noted that, this approximation is valid only if the term associated with $P_t^{aux,sop,k}$ appears with negative sign in the objective function. Equation (5.44) can be re-written as follows.

$$P_t^{sop,k}(sin\theta_h^{'}-sin\theta_h)+Q_t^{sop,k}(cos\theta_h-cos\theta_h^{'})+P_t^{aux,sop,k}sin(\theta_h-\theta_h^{'}) \leq 0 \quad h \in [1,H] \tag{5.46}$$

$$P_t^{loss,sop,k} = A^{sop,k}P_t^{aux,sop,k} \tag{5.47}$$

5.4 Methodology

5.4.1 MGO model based on Info-gap decision theory

The uncertainty in RESs power presents several challenges in decision making in energy management. The uncertainty can be dealt with different methods such as probabilistic approach, fuzzy theory based approach, robust optimization, and Information-Gap Decision Theory (IGDT) [137]. Unlike other methods, IGDT does not require large amounts of historical data to extract information about Probability Density Functions (PDFs), membership functions, exact uncertainty sets, etc. The aim of IGDT is to make optimal decisions to maximize the robustness of the objective function against the uncertainty of the input parameters. In this work, IGDT based model is used to deal with uncertainties associated with RESs. IGDT assists in decisions-making under uncertainty without requiring the PDF of uncertain parameters. Two different strategies, robust (risk-averse decision making) and opportunistic (risk-seeker decision making), can be adopted by the decision-maker to deal with uncertainty. The robust model of IGDT estimates the highest tolerable level of uncertainty, while the opportunistic model determines the lowest level of uncertainty required for targeted windfall profit [138]. In this work, it is assumed that the only available information is the forecasted value of the RESs power, $\bar{P}_t^{RES,m}$. The uncertainty set of RESs power $\Gamma(\alpha^m, \bar{P}_t^{RES,m})$ to describe the behavior of uncertain parameter, $P_t^{RES,m}$ can be modeled as

$$\Gamma(\alpha^m, \bar{P}_t^{RES,m}) = \left\{ P_t^{RES,m} : \left| \frac{P_t^{RES,m} - \bar{P}_t^{RES,m}}{\bar{P}_t^{RES,m}} \right| \leq \alpha^m \right\}. \tag{5.48}$$

Here, α^m is the uncertainty level. From (5.48), the range of uncertain value of RESs power can be defined as

$$P_t^{RES,m} = (1 \pm \alpha^m)\bar{P}_t^{RES,m}. \tag{5.49}$$

The profit of MGO decreases (increases) as the power of RESs decreases (increases). The highest level of uncertainty to achieve minimum targeted profit can be determined with lower bound of the RESs power, $(1-\alpha^m)\bar{P}_t^{RES,m}$, while the minimum level of uncertainty to obtain targeted windfall profit can be determined with upper bound of RESs power, $(1+\alpha^m)\bar{P}_t^{RES,m}$. Therefore, plus and minus signs in Equation (5.49) are used for risk-seeker and risk-averse strategies, respectively. The MGO level problem can be reformulated for risk-averse and risk-seeker modeling as follows.

Risk-averse model:

$$\begin{aligned} &max \quad \alpha^m \\ &F_{MGO,ra}^m \geq (1-\gamma_{ra})F_{MGO,0}^m, \\ &P_t^{RES,m} = (1-\alpha^m)\bar{P}_t^{RES,m}, \\ &constraints \quad (5.21)-(5.28). \end{aligned}$$

Risk-seeker model:

$$\begin{aligned} &min \quad \alpha^m \\ &F_{MGO,rs}^m \geq (1+\gamma_{rs})F_{MGO,0}^m, \\ &P_t^{RES,m} = (1+\alpha^m)\bar{P}_t^{RES,m}, \\ &constraints \quad (5.21)-(5.28). \end{aligned}$$

Here, $F_{MGO,0}^m$ is the profit of MGO based on the forecasted value of the RESs power, i.e., when the optimization problem discussed in the section 5.3.2 is solved assuming $P_t^{RES,m}$ equals to the forecasted value, $\bar{P}_t^{RES,m}$. γ_{ra} and γ_{rs} are the parameters set by decision-maker within the range of 0 to 1.

5.4.2 Solution approach for three-level optimization

In the proposed energy management framework, multiple decision-making is performed by several agents at three levels. The EUAs schedule their assets, viz. DR loads, BESSs, and PHEVs to maximize their profits on a tariff proposed by an MGO. The EUAs and MGO

interact with each other using a bi-level leader-follower approach. MGO acts as a leader, and EUAs act as followers in the lower level game. This lower bi-level problem can be rephrased as a Mathematical Problem with Equilibrium Constraints (MPEC) [139] for each MGO. Optimization problems of all the EUAs can be replaced by their first-order Karush-Kuhn-Tucker (KKT) optimality conditions along with equality constraints and complementarity conditions in order to get the MPEC formulation. This solution approach of converting a bi-level problem into an equivalent single-level optimization problem relies on the fact that if the follower's optimization problems constraining the leader optimization problem are convex, they can be replaced by their respective KKT conditions. This solution approach can not be directly used if the optimization problems of the followers are non-convex. All lower-level MPECs of all MGOs can be solved in parallel. The outcomes of individual lower-level MPEC are scheduled DR loads, PHEVs and BESSs demand patterns, power exchange requests of EUAs with their respective MGOs, MGOs' offered tariffs to EUAs, and the uncertainty level of RESs power. The first-order KKT optimality conditions of EUAs can be written in the following manner.

$$-\rho_t^{n_B,n} - \lambda_t^{1,n} - \mu_t^{4,n_B,n} + \mu_t^{5,n_B,n} = 0 \qquad : d_t^{n_B,n} \tag{5.50}$$

$$\rho_t^m + \lambda_t^{7,n} - \mu_t^{20,n} + \mu_t^{21,n} = 0 \qquad : P_t^n \tag{5.51}$$

$$-\mu_t^{1,n} + \mu_t^{2,n} - \mu^{3,n} + \lambda_t^{1,n} - \lambda_t^{7,n} = 0 \qquad : P_t^{DR,n} \tag{5.52}$$

$$\lambda_t^{2,n} - \eta_{sd}\lambda_{t+1}^{2,n} - \mu_t^{10,n} + \mu_t^{11,n} - (1-\eta_{sd})\lambda^{3,n} = 0 \qquad : E_t^{b,n} \tag{5.53}$$

$$-\eta_c\lambda_t^{2,n} - \mu_t^{6,n} + \mu_t^{7,n} + \eta_c\lambda_t^{3,n} - \lambda_t^{7,n} = 0 \qquad : P_t^{c,b,n} \tag{5.54}$$

$$\rho^d + \frac{\lambda_t^{2,n}}{\eta_d} - \mu_t^{8,n} + \mu_t^{9,n} - \frac{\lambda_t^{3,n}}{\eta_d} + \lambda_t^{7,n} = 0 \qquad : P_t^{d,b,n} \tag{5.55}$$

$$\begin{aligned}\lambda_t^{4,ev,n}|_{t>t_{arri}} - \eta_{sd}\lambda_{t+1}^{4,ev,n} - \mu_t^{16,ev,n} + \mu_t^{17,ev,n} \\ + \lambda_t^{5,ev,n}|_{t=t_{depa}} + \lambda_t^{6,ev,n}|_{t=t_{arri}} = 0 \qquad : E_t^{ev,n}\end{aligned} \tag{5.56}$$

$$\begin{aligned}-\eta_c\lambda_t^{4,ev,n}|_{t>t_{arri}} - \mu_t^{12,ev,n} + \mu_t^{13,ev,n} - \eta_c\lambda_t^{6,ev,n}|_{t=t_{arri}} \\ - \lambda_t^{7,n} - \mu_t^{18,ev,n} + \mu_t^{19,ev,n} = 0 \qquad : P_t^{c,ev,n}\end{aligned} \tag{5.57}$$

$$\begin{aligned}\rho^d + \left.\frac{\lambda_t^{4,ev,n}}{\eta_d}\right|_{t>t_{arri}} - \mu_t^{14,ev,n} + \mu_t^{15,ev,n} + \left.\frac{\lambda_t^{6,ev,n}}{\eta_d}\right|_{t=t_{arri}} \\ + \lambda_t^{7,n} + \mu_t^{18,ev,n} - \mu_t^{19,ev,n} = 0 \qquad : P_t^{d,ev,n}\end{aligned} \tag{5.58}$$

The non-linearities associated with these complementarity constraints can be linearized by using the Fortunty-Armat method (BigM method) [140]. The complementarity conditions corresponding to EUA inequality constraints and their dual variables are represented in the Equations (5.59)-(5.79) as follows.

$$0 \leq (P_t^{DR,n} - 0.9P_t^{0,n}) \perp \mu_t^{1,n} \geq 0, \tag{5.59}$$

$$0 \leq (1.1P_t^{0,n} - P_t^{DR,n}) \perp \mu_t^{2,n} \geq 0, \tag{5.60}$$

$$0 \leq \left(\zeta \sum_{t=1}^{T} P_t^{0,n} - \sum_{t=1}^{T} \left(P_t^{0,n} - P_t^{DR,n}\right)\right) \perp \mu_t^{3,n} \geq 0, \tag{5.61}$$

$$0 \leq d_t^{n_B,n} \perp \mu_t^{4,n_B,n} \geq 0, \tag{5.62}$$

$$0 \leq (d^{max,n_B,n} - d_t^{n_B,n}) \perp \mu_t^{5,n_B,n} \geq 0, \tag{5.63}$$

$$0 \leq P_t^{c,b,n} \perp \mu_t^{6,n} \geq 0, \tag{5.64}$$

$$0 \leq (P^{cmax,b,n} - P_t^{c,b,n}) \perp \mu_t^{7,n} \geq 0, \tag{5.65}$$

$$0 \leq P_t^{d,b,n} \perp \mu_t^{8,n} \geq 0, \tag{5.66}$$

$$0 \leq (P^{dmax,b,n} - P_t^{d,b,n}) \perp \mu_t^{9,n} \geq 0, \tag{5.67}$$

$$0 \leq (E_t^{b,n} - E^{min,b,n}) \perp \mu_t^{10,n} \geq 0, \tag{5.68}$$

$$0 \leq (E^{max,b,n} - E_t^{b,n}) \perp \mu_t^{11,n} \geq 0, \tag{5.69}$$

$$0 \leq P_t^{c,ev,n} \perp \mu_t^{12,ev,n} \geq 0, \tag{5.70}$$

$$0 \leq (P^{cmax,ev,n} - P_t^{c,ev,n}) \perp \mu_t^{13,ev,n} \geq 0, \tag{5.71}$$

$$0 \leq P_t^{d,ev,n} \perp \mu_t^{14,ev,n} \geq 0, \tag{5.72}$$

$$0 \leq (P^{dmax,ev,n} - P_t^{d,ev,n}) \perp \mu_t^{14,ev,n} \geq 0, \tag{5.73}$$

$$0 \leq (E_t^{ev,n} - E^{min,ev,n}) \perp \mu_t^{16,ev,n} \geq 0, \tag{5.74}$$

$$0 \leq (E^{max,ev,n} - E_t^{ev,n}) \perp \mu_t^{17,ev,n} \geq 0, \tag{5.75}$$

$$0 \leq \left(\sum_{ev=1}^{N_{ev}} (P_t^{c,ev,n} - P_t^{d,ev,n}) + P^{evmax}\right) \perp \mu_t^{18,n} \geq 0, \tag{5.76}$$

$$0 \leq \left(P^{evmax} - \sum_{ev=1}^{N_{ev}} (P_t^{c,ev,n} - P_t^{d,ev,n})\right) \perp \mu_t^{19,n} \geq 0, \tag{5.77}$$

$$0 \leq (P_t^n + P^{max,n}) \perp \mu_t^{20,n} \geq 0, \tag{5.78}$$

$$0 \leq (P^{max,n} - P_t^n) \perp \mu_t^{21,n} \geq 0. \tag{5.79}$$

The non-linearity in the lower MPEC associated with term $P_t^n \rho_t^m$ in the objective function (5.20) can be linearized using strong duality theory. According to strong duality, the dual of EUAs objective can be written as,

$$\begin{aligned} & P_t^n \rho_t^m - \sum_{n_B=1}^{N_B} d_t^{n_B,n} \rho_t^{n_B,n} + \left(P_t^{d,b,n} + \sum_{ev=1}^{N_{ev}} P_t^{d,ev,n} \right) \rho^d = 0.9 P_t^{0,n} \mu_t^{1,n} - 1.1 P_t^{0,n} \mu_t^{2,n} \\ & + (1-\zeta) P_t^{0,n} \mu^{3,n} - \sum_{n_B=1}^{N_B} d^{max,n_B,n} \mu_t^{5,n_B,n} - P^{cmax,b,n} \mu_t^{7,n} - P^{dmax,b,n} \mu_t^{9,n} + E^{min,b,n} \mu_t^{10,n} \\ & - E^{max,b,n} \mu_t^{11,n} - P^{evmax} (\mu_t^{18,n} + \mu_t^{19,n}) + \sum_{ev=1}^{N_{ev}} \Bigg(- P^{cmax,ev,n} \mu_t^{13,ev,n} - P^{dmax,ev,n} \mu_t^{15,ev,n} \\ & + E^{min,ev,n} \mu_t^{16,ev,n} - E^{max,ev,n} \mu_t^{17,ev,n} - E_{t_{depa}}^{ev,n} \lambda_{t_{depa}}^{5,ev,n} - E_{t_{arri}}^{ev,n} \lambda_{t_{arri}}^{6,ev,n} \Bigg). \end{aligned} \tag{5.80}$$

The MGOs are intermediate players of the proposed energy management framework. They have to interact with EUAs and DU. The interaction of MGO and EUAs is considered in the lower MPEC, as discussed above. DU and MGO interact with each other in upper bi-level game. Some of the variables decided in the lower-level MPECs (i.e., power exchange requests of EUAs, MGOs' offered tariffs to EUAs, and uncertainty level) are considered as parameters in the upper-level problem. After that, the resultant MGOs' problem can be replaced by their first-order optimality conditions, equality constraints, and complementarity conditions to form a single level MPEC of bi-level optimization of DU and MGO. The first-order optimality conditions and complementarity conditions of MGOs can be written as,

$$\rho_t^{base} + \delta(2P_t^m + \sum_{-m} P_t^{-m} + P_t^{L,du}) - \mu_t^{22,m} + \mu_t^{23,m} + \lambda_t^{8,m} = 0 \qquad : P_t^m \tag{5.81}$$

$$\rho^{dg,m} + \rho^{emi} - \mu_t^{27,m} + \mu_t^{28,m} + \lambda_t^{8,m} + \mu_{t+1}^{29,m} - \mu_t^{29,m} + \mu_t^{30,m} - \mu_{t+1}^{30,m} = 0 \qquad : P_t^{dg,m} \tag{5.82}$$

$$0 \leq (P_t^m + P^{max,m}) \perp \mu_t^{22,m} \geq 0, \tag{5.83}$$

$$0 \leq (P^{max,m} - P_t^m) \perp \mu_t^{23,m} \geq 0, \tag{5.84}$$

$$0 \leq P_t^{dg,m} \perp \mu_t^{27,m} \geq 0, \tag{5.85}$$

$$0 \leq (P^{DGmax,m} - P_t^{dg,m}) \perp \mu_t^{28,m} \geq 0, \tag{5.86}$$

$$0 \leq (RD^{dg,m} - P_{t-1}^{dg,m} + P_t^{dg,m}) \perp \mu_t^{29,m} \geq 0, \tag{5.87}$$

$$0 \leq (RU^{dg,m} - P_t^{dg,m} + P_{t-1}^{dg,m}) \perp \mu_t^{30,m} \geq 0. \tag{5.88}$$

The outcomes of upper MPEC are output powers of dispatchable DGs of DU and MGOs, power exchange request of DU to the main grid, power exchange requests of the MGOs to the DU, and power exchange price between DU and MGOs. A common optimal solution of all levels can be achieved by solving upper and lower level MPECs iteratively. As stated above, the DU has two objectives, i.e., cost minimization and voltage deviation minimization. The ε-constraint method [121] is used to solve the upper MPEC. The solution approach is summarized in the flow chart given in Figure 5.4.

5.5 Results and discussion

5.5.1 System description

In this study, IEEE 33-bus distribution system shown in the Figure 5.5 has been considered to implement and evaluate the efficacy of the proposed method. The distribution system consists of three MGs, two dispatchable DGs (MTs), two SOPs, and consumer loads connected at each bus. The PCC with the main grid is present at bus 1. The MG1, MG2, and MG3 are connected at bus numbers 21, 24, and 30, respectively. The dispatchable DGs with 0.8 p.u. capacities are present at the 6th and 13th buses. The bus number 18 and 33 are connected through SOP1, while 25 and 29 are connected through SOP2. The kVA rating of each of the SOPs is 1.0 p.u. The main grid power exchange price and total consumer load of DU are shown in Table 5.1.

The rated capacities of dispatchable DGs (MTs) are 1.0 p.u. for MG1 and 0.8 p.u. for MG2 and MG3. The operating cost coefficients of the dispatchable DGs are assumed

Table 5.1: Main grid tariff and DU's consumer load

Hour	1	2	3	4	5	6	7	8	9	10	11	12
ρ_t^g (€/kWh)	0.071	0.063	0.058	0.053	0.054	0.061	0.071	0.085	0.087	0.095	0.105	0.113
$P_t^{L,du}$ (p.u.)	2.274	2.241	2.195	2.187	2.179	2.186	2.300	2.531	2.814	3.060	3.191	3.226
Hour	13	14	15	16	17	18	19	20	21	22	23	24
ρ_t^g (€/kWh)	0.112	0.120	0.132	0.144	0.150	0.144	0.142	0.126	0.129	0.127	0.114	0.093
$P_t^{L,du}$ (p.u.)	3.176	3.140	3.100	3.037	2.953	2.918	2.878	2.855	2.782	2.641	2.487	2.345

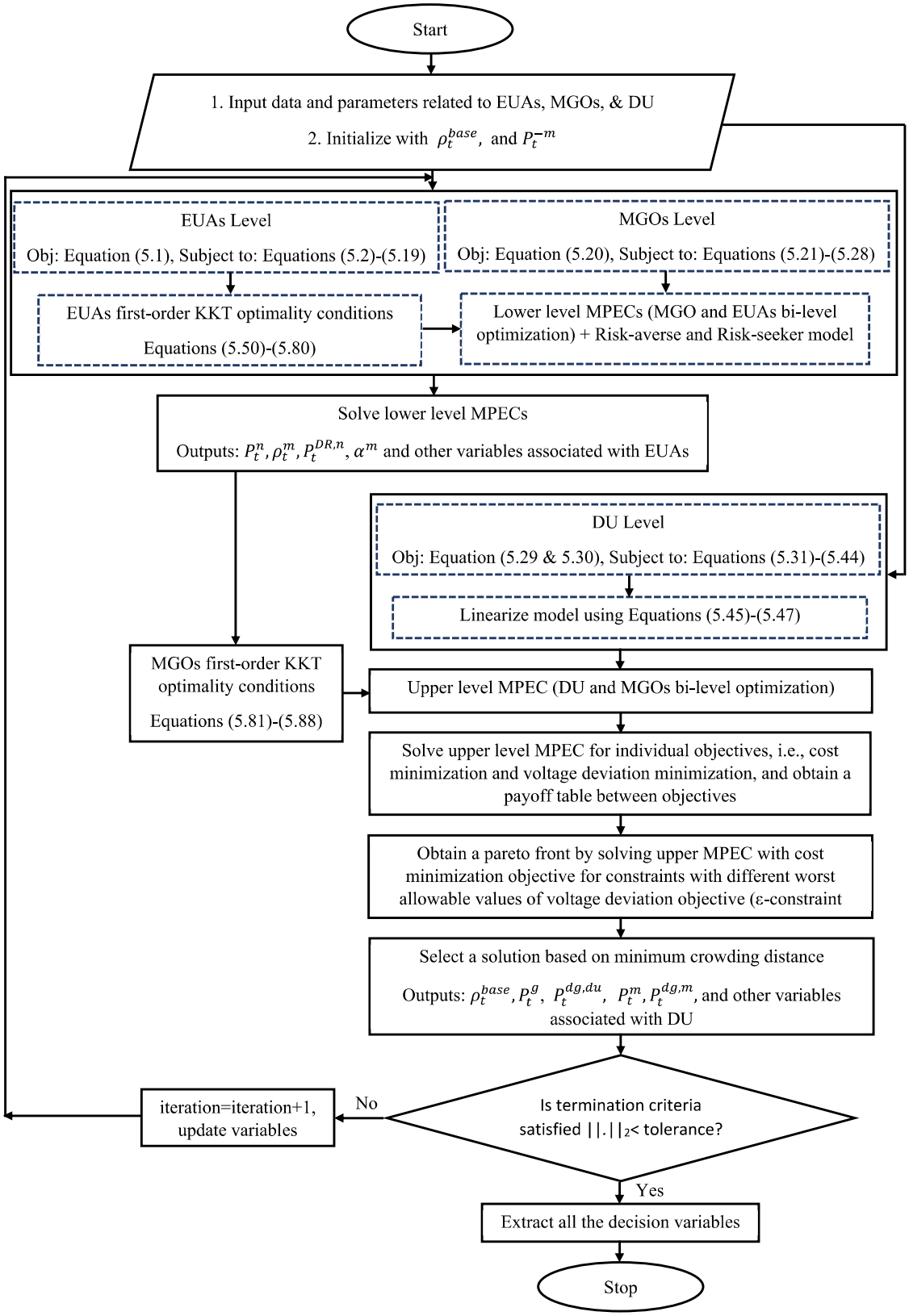

Figure 5.4: Energy management framework flow chart

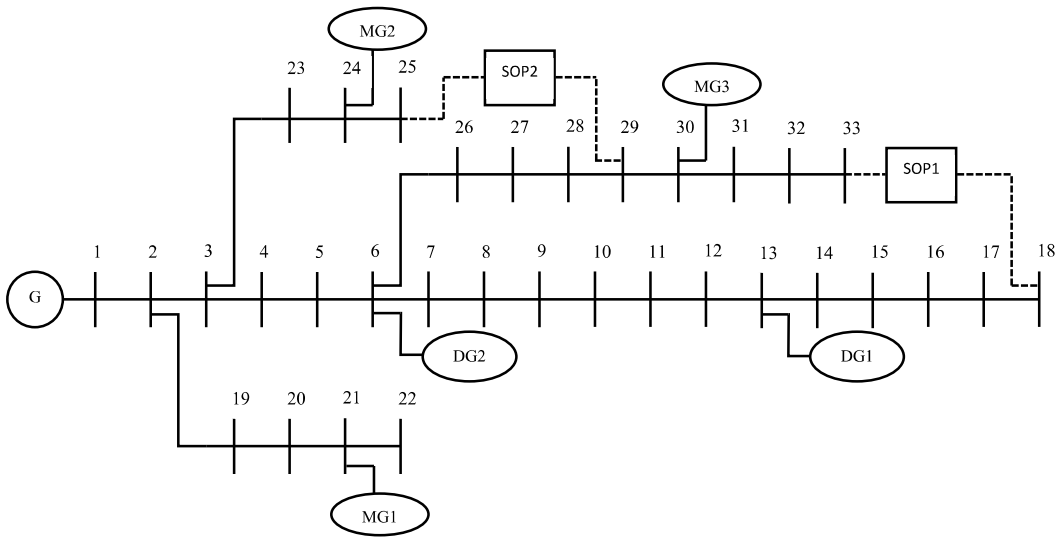

Figure 5.5: IEEE 33-bus test system

to be 0.12 €/kWh for DU, and 0.108, 0.116 and 0.112 €/kWh for MG1, MG2, and MG3, respectively. The greenhouse gas emission cost coefficient, ρ^{emi} is 0.017 €/kWh. Each MG has eight EUAs in its premises with $P^{max,n}$ ratings in the range 0.35 to 1.2 p.u. The RESs rated capacities for the MG1, MG2, and MG3 are 3.5, 4.0 and 3.0 p.u., respectively. The forecasted RESs power and total demand of EUAs before DR are shown in Figure 5.6. Each EUA has BESS with Battery Capacity (BC) equal to 25% of its rated power. The NHTS 2017 datasets [**?**] has been used to generate parameters of the PHEVs. The minimum and maximum energy levels of BESSs and PHEVs are considered as 10% and 90% of their respective BCs. The charging and discharging efficiencies of the battery chargers are assumed to be 95%. In this work, the self-discharge of the batteries is assumed to be negligible[1] (i.e., $\eta_{sd} = 1$). The maximum shifting limit of DR load is assumed to be $\pm$10% of load demand in a time interval. The maximum limit of load curtailment is 5% of total DR load in 24 hours interval. The step-wise DR price curve data is given in Table 5.2. Scaling factors of 1.2 for time interval 7:00-15:00 hours and 1.4 for time interval 16:00-24:00 hours are used to convert price data in Table 5.2 to TOU price. The GAMS/CPLEX solver is used to perform the simulations.

[1]If it is assumed that the self-discharge rate of the battery is 10% for one day, then η_{sd} will be equal to $\sqrt[24]{0.90}$ for an interval of 1 hour.

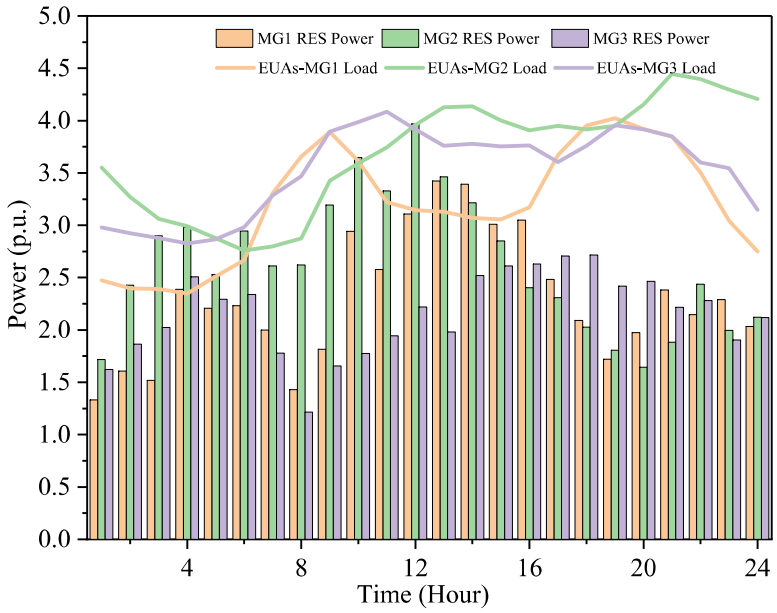

Figure 5.6: RESs power and EUAs total demand of MGs

Table 5.2: Stepwise price curve data for EUA

Rated power	$d^{1,n}$	$d^{2,n}$	$d^{3,n}$	$d^{4,n}$	$\rho_{\cdot}^{1,n}$	$\rho_{\cdot}^{2,n}$	$\rho_{\cdot}^{3,n}$	$\rho_{\cdot}^{4,n}$
0.3	0.05	0.05	0.1	0.1	0.112	0.104	0.102	0.092
0.4	0.1	0.1	0.1	0.1	0.112	0.104	0.102	0.092
0.7	0.1	0.1	0.2	0.3	0.118	0.112	0.104	0.094
0.8	0.1	0.2	0.2	0.3	0.118	0.112	0.104	0.094
0.9	0.1	0.2	0.3	0.3	0.128	0.122	0.112	0.104
1	0.1	0.2	0.3	0.4	0.128	0.122	0.112	0.104
1.1	0.2	0.2	0.3	0.4	0.128	0.122	0.112	0.104
1.2	0.2	0.3	0.3	0.4	0.128	0.122	0.112	0.104

5.5.2 Game-theoretic pricing based energy management

Three different cases used to demonstrate the effectiveness of the proposed three-level EMS are as follows.

Case I: This is considered as a base case. In this case, all the MGOs and EUAs interact, and the tariff for EUAs is decided by using the internal game between MGO and EUAs. The DU provides a base price ρ_t^{base} (same as ρ_t^g given in Table 5.1) to the MGOs for power exchange with distribution system. The lower level MPECs are solved iteratively to achieve equilibrium stage of all the strategies of all MGOs and provide their power exchange requests to DU. Finally, the DU optimizes its assets based on power exchange requests received from MGOs.

Case II: The proposed EMS is used in this case study. The tariff of DU and tariffs of MGOs are decided using the three-level game. For comparative analysis, the average value of base price, $\rho^{avg,base}$, is assumed to be the same as the average value of ρ_t^g. The uncertainties associated with RESs are not included in this case.

Case III: This is similar to *Case II*, and the IGDT model is used to consider the uncertainties associated with RESs. All other parameters are the same as in *Case II*.

After simulation of *Case I* and *Case II*, the results are analyzed as follows. The prices offered by MGOs to EUAs and the base price offered by DU to MGOs are shown in Figure 5.7. The MGOs adjust the tariff according to the demand pattern of EUAs using bi-level optimization. The base price offered by DU to MGOs also affects the prices offered by MGO to EUAs. The time interval 1:00-8:00 hours is the low tariff period. It is observed that based on EUAs' demand profile, all the MGOs have different tariffs for their respective EUAs. The tariff obtained in *Case I* and *Case II* are different. This difference in the prices offered by MGO in *Case I* and *Case II* is due to different base prices, ρ_t^{base}. The EUAs power exchange with MGOs is depicted in Figure 5.8. During 1:00-14:00 hours, the power exchange in both the cases is almost identical for all the MGs. The power demands of EUAs in MG2 and MG3 shift from 15:00-16:00 hours to 17:00-22:00 hours. The MGOs offered prices have the same pattern in both cases during these hours. But the base price offered by DU has lower value after 16:00 hours in *Case II*. So, the MGO tends to import more power after 16:00 hours. The power exchange of MGO with DU depends on the EUAs' power demand. Therefore, this change in EUAs' power demand is beneficial for the MGO without significantly affecting the cost of EUAs.

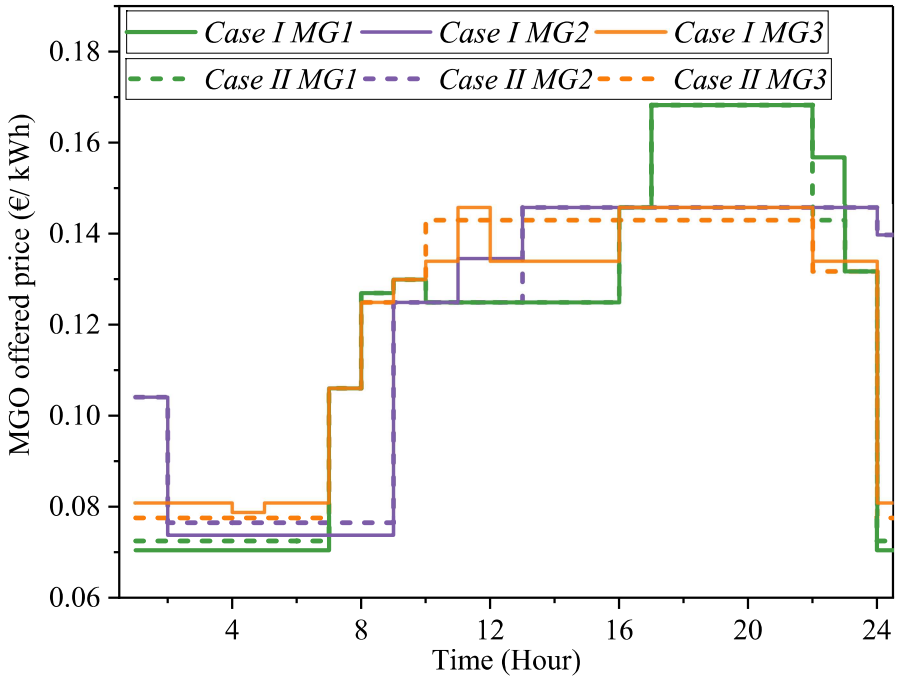

(a)

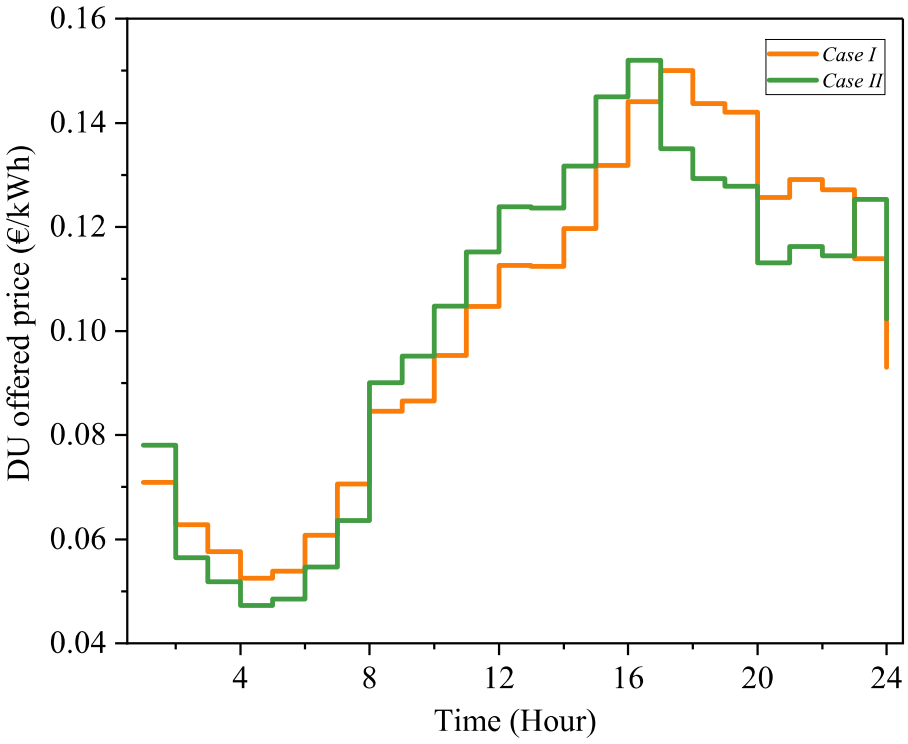

(b)

Figure 5.7: Offered prices (a) MGO offered price to EUAs, (b) Base price offered by DU

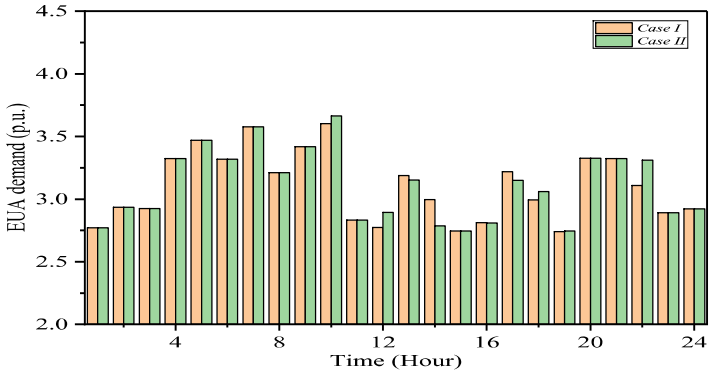

(a)

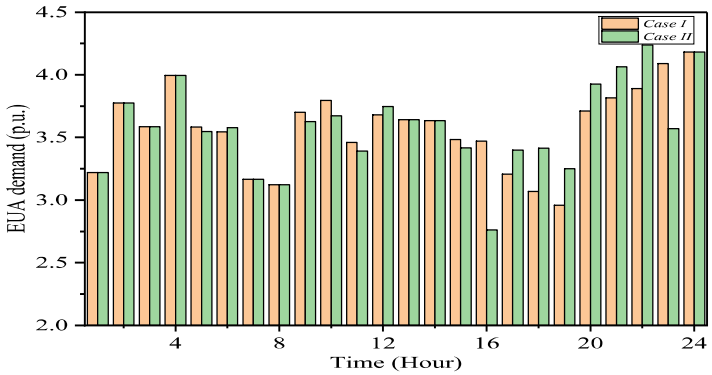

(b)

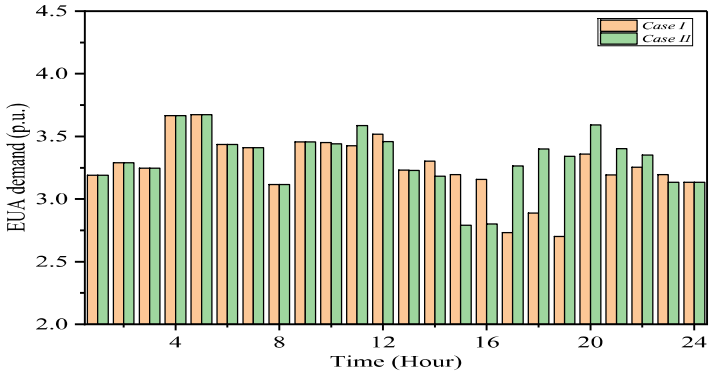

(c)

Figure 5.8: EUAs' power exchange with MGOs (a) MG1, (b) MG2, (c) MG3

The EUAs schedule their BESSs and PHEVs according to the MGO tariff to earn the maximum benefit. The scheduled demand of PHEVs and BESSs is shown in Figure 5.9. From 17:00 hours onwards, the discharging power is staggered in time in both the cases, *Case I* and *Case II*. The net power demand of EUAs decreases as the discharging power of PHEVs and BESS increases. For example, EUAs power demands in MG2 and MG3 have lower values at 16:00 hours due to high discharging power in *Case II* as compared to *Case I*. Similarly, EUAs power demands in MG2 and MG3 have higher values during 17:00-19:00 hours due to low discharging power in *Case II* as compared to *Case I*.

The decision making at all the three levels are inter-related in *Case II*. The power demand of EUAs affects the power exchange of the MGO with DU, or indirectly DU tariff to MGO and MGO tariff to EUAs. The power exchange of MGOs with DU is depicted in Figure 5.10. The MGOs' power import reduces by 5.653% in *Case II* as compared to *Case I*. DU changes its tariff according to the MGOs' demand, and in turn, MGOs change their tariffs for EUAs. The EUAs change their demand as discussed above. Also, the power exchange of MGO depends on generation availability and demand response limits. MG1 and MG3 have low RESs power output and high demand during 7:00-9:00 hours, so they need to import more power from DU to satisfy their consumer demands. The MGOs increase the output of dispatchable DGs as they receive higher price for power export to DU in *Case II*. The total power export increases from 7.975 p.u. to 11.361 p.u. in *Case II* as compared to *Case I*.

The proposed framework is beneficial to DU both from economic and technical points of view. The Figure 5.11 shows that the total power demand of DU reduces in *Case II* as compared to *Case I*. The peak demand decreases from 6.584 p.u. (*Case I*) to 6.343 p.u. (*Case II*) and the net power import decreases by 16.27% in *Case II*, and consequently, the minimum voltage level increases from 0.948 p.u. to 0.968 p.u. The voltage magnitude profile of the IEEE 33-bus system is shown in Figure 5.12. The under voltage occurs mainly during 1:00-13:00 hours and 20:00-24:00 hours because power import from the main grid is high during these time intervals as shown in Figure 5.11. The power exchange request by MGs affects the voltage level in the distribution system. For example, the voltage levels are at the lowest level at Bus No. 24 and 25 at 1:00, 2:00, and 24:00 hours due to the high power demand by MG2. The minimum voltage profile during a day is shown in Figure 5.13. The value of the voltage deviation index, F_{DU}^{V}, decreases from 9.768

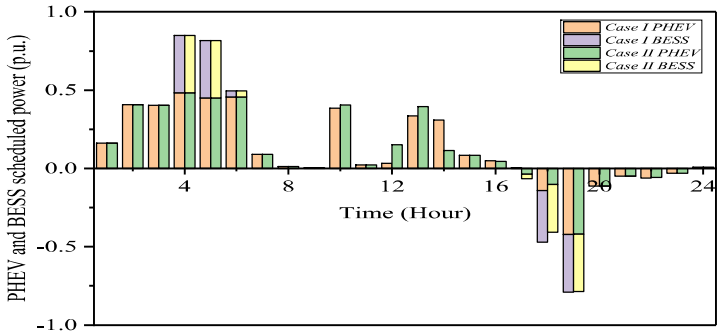

(a)

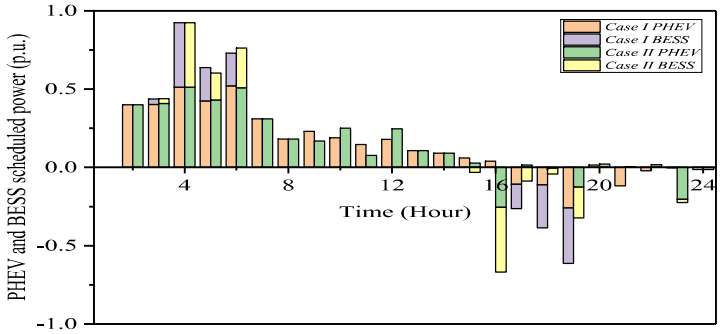

(b)

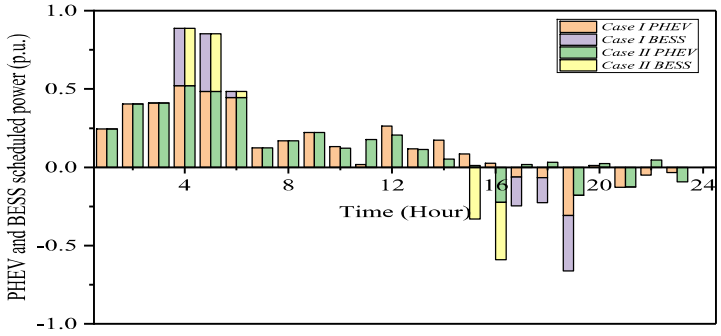

(c)

Figure 5.9: Scheduled power for PHEVs and BESSs (a) MG1, (b) MG2, and (c) MG3. The positive values refer to the charging power while the negative values refer to the discharging power.

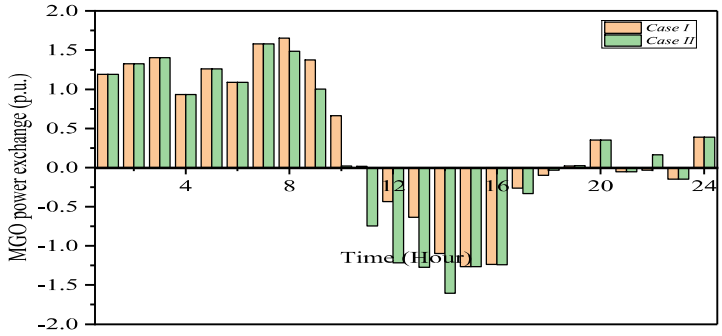

(a)

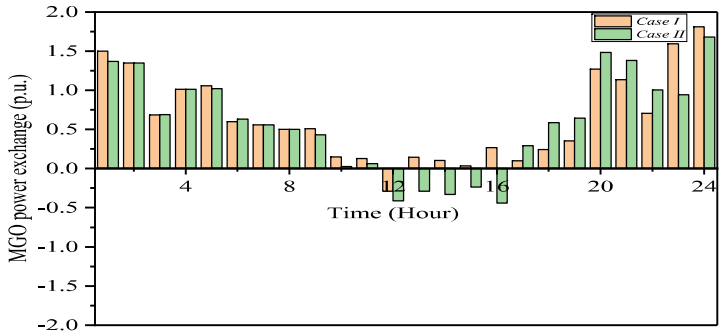

(b)

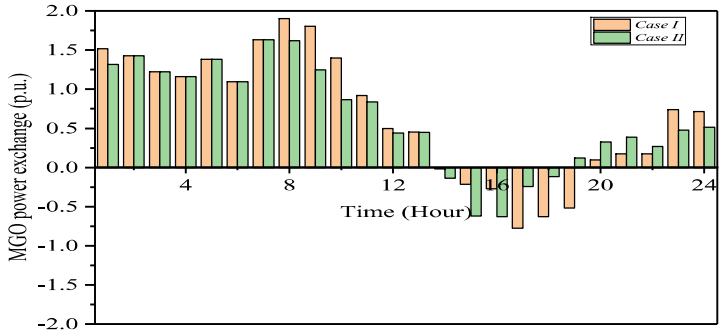

(c)

Figure 5.10: MGOs' power exchange with DU (a) MG1, (b) MG2, and (c) MG3. The positive values refer to the import while the negative values refer to the export.

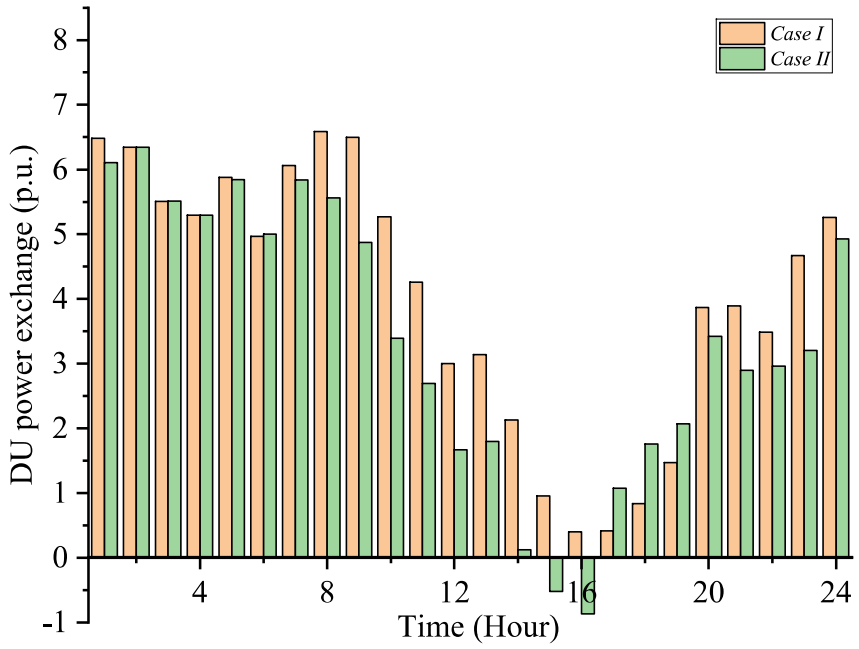

Figure 5.11: DU power exchange with the main grid

to 6.090 in *Case II* as compared to *Case I*. The sample load flow results for IEEE 33-bus system for 20:00 hours are provided in Table 5.3.

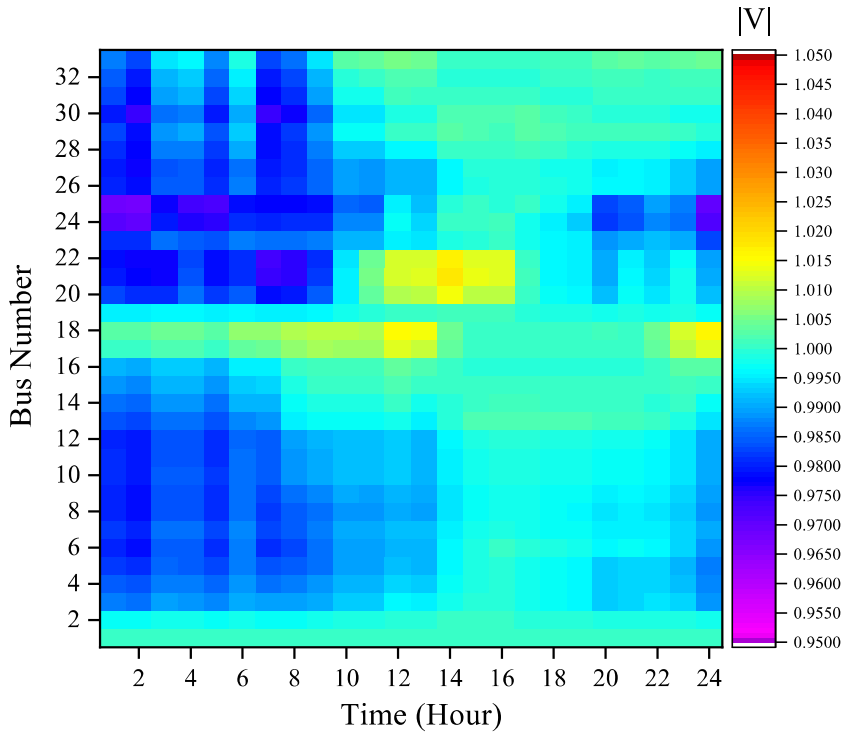

Figure 5.12: Voltage level of IEEE 33-bus system

Table 5.3: IEEE 33-Bus system power flow results for t=20:00 Hour

Bus	P (p.u.)	Q (p.u.)	V (p.u.)
1	0.000	0.000	1.000
2	1.125	0.675	0.999
3	0.808	0.359	0.993
4	1.047	0.698	0.993
5	0.675	0.337	0.993
6	0.538+0.8*	0.180	0.996
7	1.746	0.873	0.995
8	1.746	0.873	0.995
9	0.539	0.180	0.996
10	0.524	0.175	0.997
11	0.393	0.262	0.997
12	0.675	0.394	0.998
13	0.523+0.8*	0.306	1.001
14	1.350	0.900	1.000
15	0.539	0.180	1.000
16	0.524	0.175	1.000
17	0.524	0.175	1.001
18	0.808	0.359	1.001
19	1.012	0.450	0.998
20	0.786	0.349	0.992
21	0.353#	0.000	0.991
22	1.012	0.450	0.990
23	0.786	0.436	0.989
24	1.483#	0.000	0.982
25	3.666	1.746	0.983
26	0.524	0.218	0.996
27	0.539	0.224	0.996
28	0.524	0.175	0.999
29	1.047	0.611	1.001
30	0.328#	0.000	0.999
31	1.687	0.787	1.000
32	2.362	1.125	1.001
33	0.524	0.349	1.003

∗ DG power # MG power

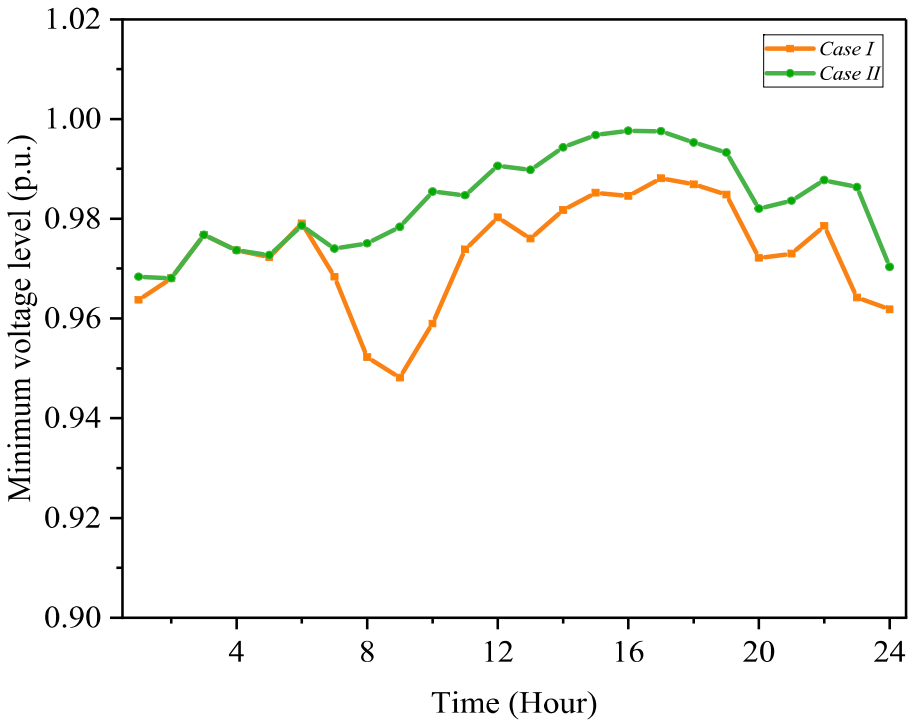

Figure 5.13: Minimum voltage profile

The profit comparison of all case studies is presented in Table 5.4. The EUAs' sum total profit is almost same in *Case I* and *Case II* for all the MGs. The MGO tariff for EUAs is decided based on the bi-level game between MGO and EUAs in both the cases. In *Case II*, the MGOs participate in DU tariff update and decide their own tariff for EUAs. The MGOs profits increase from 6899.123 € (MG1) and 7535.708 € (MG2) to 6973.705 € (MG1) and 7582.320 € (MG2) for MG1 and MG2, respectively. The profit of MG3 slightly decreases from 6382.848 € (*Case I*) to 6371.247 € (*Case II*). The total increment in MGO profit depends on their surplus energy. For example, MG1 has a maximum increase in the profit because MG1 is able to export more power than other MGs. The operating cost of DU, F_{DU}^{C}, decreases from 1530.423 € (*Case I*) to 1273.087 € (*Case II*).

5.5.3 Impact of risk-averse and risk-seeker decision making of MGOs on the cost of DU

The operating cost of DU increases as the risk-averse parameter increases due to higher power demand by MGOs, whereas for risk-seeking decision making, the operating cost

Table 5.4: Comparison of all case studies

	Case I	*Case II*	*Case III*			
			risk-averse		risk-seeker	
			$\gamma_{ra} = 0.05$	$\gamma_{ra} = 0.10$	$\gamma_{rs} = 0.05$	$\gamma_{rs} = 0.10$
$\sum_{n \in MG1} F^n_{EUA}$	717.957	717.784	721.910	730.176	716.226	720.446
$\sum_{n \in MG2} F^n_{EUA}$	1233.901	1233.562	1233.685	1233.901	1233.738	1238.754
$\sum_{n \in MG3} F^n_{EUA}$	764.539	762.435	768.239	779.257	766.776	765.736
F^1_{MGO}	6899.123	6973.705	6583.132	6251.567	7321.259	7666.025
F^2_{MGO}	7535.708	7582.320	7182.204	6798.976	7973.356	8362.315
F^3_{MGO}	6382.848	6371.247	6012.158	5685.866	6699.376	7032.059
F^C_{DU}	1530.423	1273.087	1651.892	2266.196	749.145	224.371

Table 5.5: Uncertainty levels for different strategies in *Case III*

	risk-averse		risk-seeker	
	$\gamma_{ra} = 0.05$	$\gamma_{ra} = 0.10$	$\gamma_{rs} = 0.05$	$\gamma_{rs} = 0.10$
MG1	0.04935	0.09673	0.05121	0.10406
MG2	0.04805	0.09498	0.04903	0.09944
MG3	0.04747	0.09283	0.04941	0.09971

of DU decreases as the risk-seeker parameter increases due to lower power demand by MGOs. For risk-averse decision with parameter, γ_{ra} taking values equal to 0.05 and 0.10, the operating costs of DU are 1651.892 € and 2266.196 €. Similarly, the DU cost decreases to 749.145 € and 224.371 € for risk-seeking decision with parameter, γ_{rs} taking values equal to 0.05 and 0.10, respectively. The tolerable uncertainty levels for risk-averse strategies and the lowest uncertainty level required for risk-seeker strategies are shown in Table 5.5.

5.5.4 Validation of proposed approach on unbalanced distribution system

To validate the proposed framework for an unbalanced distribution system, cases of 25-bus unbalanced distribution system [141] and modified IEEE 123-bus unbalanced distribution [142] have also been studied. The DU level power flow model has been reformulated as the three-phase power flow model [143] (given in Appendix I) to implement the proposed framework on an unbalanced distribution system.

25-bus unbalanced distribution system

For 25-bus unbalanced distribution system (shown in Appendix II), the load and generation data is considered similar to IEEE 33-bus system. The MG1, MG2, and MG3 are connected at bus number 5-A, 13-B, and 17-C, respectively. The dispatchable DGs are present at buses 7-C and 11-B. The two SOPs of 1.5 p.u. rated power are connected between bus pairs 8-15 and 12-25. The total consumer load of DU shown in Table 5.1 is distributed among three-phases of 25-buses in the ratio assumed in [141] (also given in Appendix II). A sample three-phase power flow results for the 25-bus system for 20:00 hours is given in Table 5.6. The outcomes of the unbalanced distribution system case study are shown in Table 5.7. There are small differences in the values of F^n_{EUA}, F^m_{MGO}, and F^C_{DU} for a 25-bus unbalanced distribution system compared to the results for the IEEE 33-bus system for *Case II* (Table 5.4). Although all resources and parameters are the same for both systems, the difference in the values of F^n_{EUA}, F^m_{MGO}, and F^C_{DU} is due to the offered price. The DU and MGOs offered prices for 25-bus system are shown in the Figure 5.14. DU has changed its offered base price to adjust the MGOs power exchange request to meet the economic aspect (i.e., energy cost minimization) and the technical aspect (i.e., voltage deviation minimization). Figure 5.15 shows the voltage level of three phases of the 25-bus unbalanced distribution system. Similar to the IEEE 33-bus, the voltage level of the 25-bus system depends on the MGs' demand and their phase connection. For example, buses 5-A, 13-B, and 17-C experience minimum voltage levels because MGs are connected to these buses. The MGOs' offered price to EUA, and scheduled power has also changed according to offered base price of DU and other MGO power exchange profiles. The power exchange profiles of DU, MGOs, and EUAs can be

explained in a similar manner as discussed for IEEE 33-bus system.

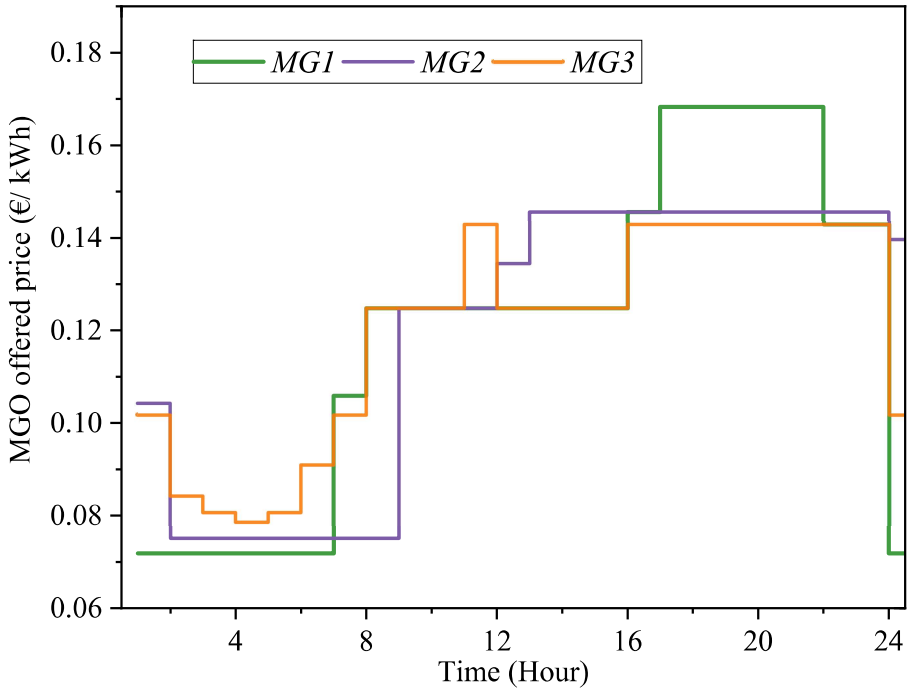

(a)

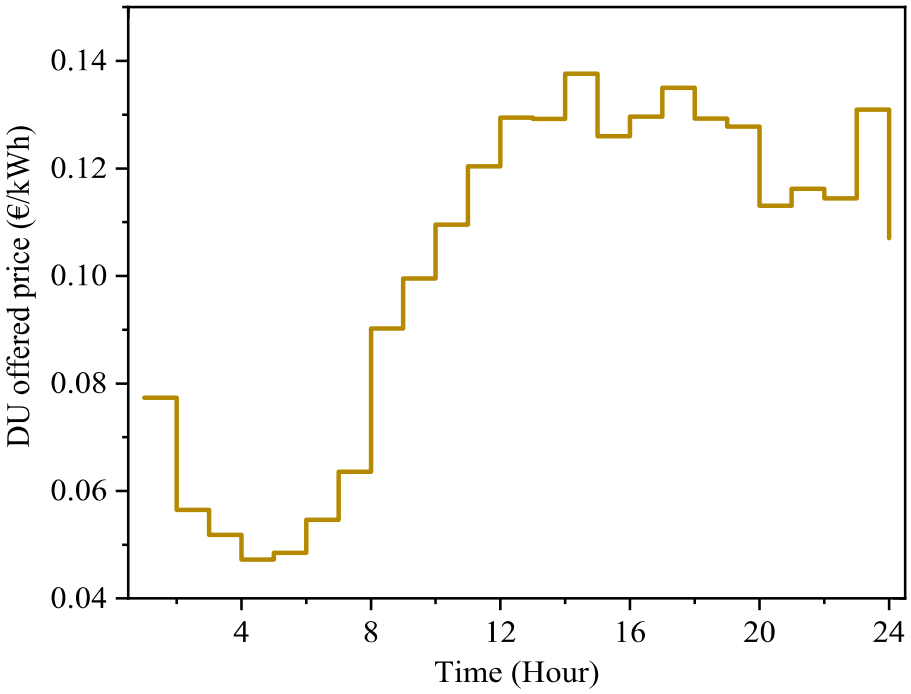

(b)

Figure 5.14: Offered prices for 25-bus system (a) MGOs' offered price to EUAs, (b) Base price offered by DU

Table 5.6: 25-Bus system power flow results for t=20:00 Hour

	P (p.u.)			Q (p.u.)			V (p.u.)		
	A	B	C	A	B	C	A	B	C
1	0.000	0.000	0.000	0.000	0.000	0.000	1.000	1.000	1.000
2	0.000	0.000	0.000	0.000	0.000	0.000	0.999	1.002	1.001
3	0.410	0.328	0.479	0.171	0.152	0.209	0.996	1.000	0.999
4	0.656	0.547	0.547	0.342	0.266	0.238	0.995	1.000	0.999
5	0.512+0.353$^{\#}$	0.342	0.427	0.238	0.158	0.198	0.988	0.999	0.998
6	0.513	0.399	0.356	0.238	0.198	0.248	0.999	0.998	1.000
7	0.000	0.000	0.240*	0.000	0.000	0.000	0.999	0.994	1.000
8	0.492	0.328	0.041	0.228	0.152	0.019	1.000	1.002	1.000
9	1.057	0.564	0.705	0.515	0.294	0.306	0.997	0.984	0.999
10	0.427	0.342	0.498	0.178	0.158	0.218	0.999	0.975	1.000
11	0.740	0.352+0.680*	0.529	0.323	0.147	0.245	1.000	0.970	1.001
12	0.656	0.547	0.547	0.285	0.266	0.285	1.004	0.976	1.003
13	0.769	0.398+1.483$^{\#}$	0.427	0.178	0.174	0.198	0.999	0.950	1.000
14	0.656	0.438	0.684	0.285	0.228	0.333	1.001	0.999	0.997
15	0.085	0.057	0.071	0.036	0.024	0.030	1.003	1.004	1.001
16	0.684	0.046	0.570	0.036	0.238	0.297	0.997	0.993	0.998
17	0.085	0.493	0.793+0.325$^{\#}$	0.441	0.245	0.392	1.000	0.998	0.989
18	0.656	0.438	0.547	0.342	0.228	0.285	0.991	0.995	0.995
19	0.127	0.070	0.088	0.066	0.034	0.049	0.989	0.994	0.993
20	0.574	0.438	0.615	0.285	0.228	0.304	0.989	0.994	0.993
21	0.068	0.399	0.064	0.036	0.020	0.032	0.988	0.992	0.992
22	0.820	0.656	0.684	0.399	0.342	0.380	0.985	0.990	0.990
23	0.103	0.057	0.712	0.535	0.032	0.347	0.997	0.999	0.999
24	0.574	0.492	0.055	0.285	0.243	0.029	1.000	0.999	1.000
25	0.098	0.547	0.068	0.051	0.023	0.033	1.007	1.000	1.002

$*$ DG power # MG power

Table 5.7: *Case II* outcomes for 25-bus unbalanced distribution system

	MG1	MG2	MG3	DU
$\sum_n F^n_{EUA}$	721.910	1233.790	774.173	-
F^m_{MGO}	6956.319	7576.582	6337.357	-
F^C_{DU}	-	-	-	1297.531

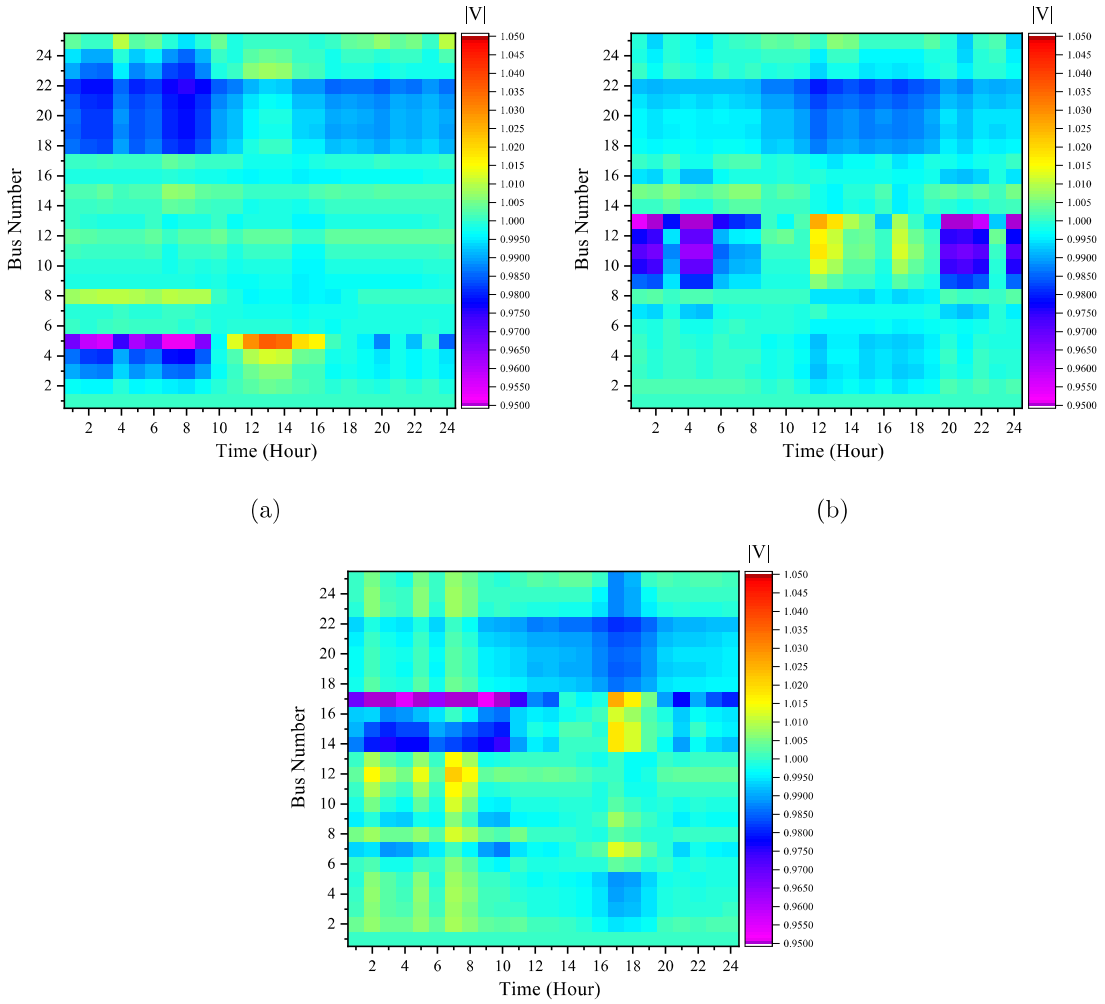

Figure 5.15: Voltage level of IEEE 25-bus system (a) Phase-A, (b) Phase-B, (c) Phase-C

Modified IEEE 123-bus unbalanced distribution system

For modified IEEE 123-bus unbalanced distribution system; base load, line data, on/off shunt capacitors data and other system related data have been considered as given in [142] with some approximations (all loads are considered as PQ load) (see Appendix II). The total consumer load of DU shown in Table 5.1 is distributed among three-phases of IEEE 123-bus system. Five MGs (MG1, MG2, MG3, MG4 and MG5) are considered in this case study. The load and generation data for MG1, MG2, and MG3 are considered same as in case of IEEE 33-bus distribution system. Whereas, the data for MG4 and MG5 was created using combinations of data for MG1, MG2 and MG3. The MG1, MG2,

MG3, MG4, and MG5 are connected at bus number 90-B, 11-A, 32-C, 6-C, and 107-B, respectively. The dispatchable DGs are present at buses 13-C and 97-B. The SOP of 1.5 p.u. rated power is connected between bus pair 151-300. A sample three phase power flow results for 25-bus system for 20:00 hours is given in Table 5.8. The outcomes of IEEE 123-bus unbalanced distribution system case study is shown in Table 5.9.

Table 5.8: IEEE 123-Bus system power flow results for t=20:00 Hour

	P			Q			V		
	A	B	C	A	B	C	A	B	C
1	0.327	0.000	0.000	0.164	0.000	0.000	0.993	0.980	0.981
2	0.000	0.164	0.000	0.000	0.082	0.000	0.000	1.000	0.000
3	0.000	0.000	0.000	0.000	0.000	0.000	0.000	0.000	0.999
4	0.000	0.000	0.327	0.000	0.000	0.164	0.000	0.000	1.000
5	0.000	0.000	0.164	0.000	0.000	0.082	0.000	0.000	1.000
6	0.000	0.000	0.327+0.974#	0.000	0.000	0.164	0.000	0.000	1.000
7	0.164	0.000	0.000	0.082	0.000	0.000	0.994	0.986	0.988
8	0.000	0.000	0.000	0.000	0.000	0.000	0.995	0.991	0.993
9	0.327	0.000	0.000	0.164	0.000	0.000	0.983	0.000	0.000
10	0.164	0.000	0.000	0.082	0.000	0.000	1.000	0.000	0.000
11	0.327+1.269#	0.000	0.000	0.164	0.000	0.000	0.989	0.000	0.000
12	0.000	0.164	0.000	0.000	0.082	0.000	0.000	0.991	0.000
13	0.000	0.000	0.24*	0.000	0.000	0.000	0.999	0.997	1.001
14	0.000	0.000	0.000	0.000	0.000	0.000	1.000	0.000	0.000
15	0.000	0.000	0.000	0.000	0.000	0.000	0.000	0.000	1.000
16	0.000	0.000	0.327	0.000	0.000	0.164	0.000	0.000	0.999
17	0.000	0.000	0.164	0.000	0.000	0.082	0.000	0.000	0.999
18	0.000	0.000	0.000	0.000	0.000	0.000	1.000	1.000	1.000
19	0.327	0.000	0.000	0.164	0.000	0.000	1.000	0.000	0.000
20	0.327	0.000	0.000	0.164	0.000	0.000	1.000	0.000	0.000
21	0.000	0.000	0.000	0.000	0.000	0.000	1.000	1.000	1.000
22	0.000	0.327	0.000	0.000	0.164	0.000	0.000	1.000	0.000
23	0.000	0.000	0.000	0.000	0.000	0.000	1.000	1.000	1.000
24	0.000	0.000	0.327	0.000	0.000	0.164	0.000	0.000	0.999
25	0.000	0.000	0.000	0.000	0.000	0.000	1.000	1.000	1.001
26	0.000	0.000	0.000	0.000	0.000	0.000	1.043	0.000	0.957
27	0.000	0.000	0.000	0.000	0.000	0.000	1.043	0.000	0.957
28	0.327	0.000	0.000	0.164	0.000	0.000	1.000	1.000	1.001
29	0.327	0.000	0.000	0.164	0.000	0.000	1.000	1.000	1.000

30	0.000	0.000	0.327	0.000	0.000	0.164	1.000	1.000	1.000
31	0.000	0.000	0.164	0.000	0.000	0.082	0.000	0.000	0.956
32	0.000	0.000	0.164+0.313#	0.000	0.000	0.082	0.000	0.000	0.956
33	0.327	0.000	0.000	0.164	0.000	0.000	1.042	0.000	0.000
34	0.000	0.000	0.327	0.000	0.000	0.164	0.000	0.000	1.000
35	0.327	0.000	0.000	0.164	0.000	0.000	1.000	1.000	1.000
36	0.000	0.000	0.000	0.000	0.000	0.000	1.000	1.000	0.000
37	0.327	0.000	0.000	0.164	0.000	0.000	1.000	0.000	0.000
38	0.000	0.164	0.000	0.000	0.082	0.000	0.000	1.000	0.000
39	0.000	0.164	0.000	0.000	0.082	0.000	0.000	1.000	0.000
40	0.000	0.000	0.000	0.000	0.000	0.000	1.000	1.000	1.000
41	0.000	0.000	0.164	0.000	0.000	0.082	0.000	0.000	1.000
42	0.164	0.000	0.000	0.082	0.000	0.000	1.000	1.000	1.000
43	0.000	0.327	0.000	0.000	0.164	0.000	0.000	1.000	0.000
44	0.000	0.000	0.000	0.000	0.000	0.000	1.000	1.000	1.000
45	0.164	0.000	0.000	0.082	0.000	0.000	1.000	0.000	0.000
46	0.164	0.000	0.000	0.082	0.000	0.000	1.000	0.000	0.000
47	0.286	0.286	0.286	0.205	0.205	0.205	1.000	1.000	1.000
48	0.573	0.573	0.573	0.409	0.409	0.409	1.000	1.000	1.000
49	0.286	0.573	0.286	0.205	0.409	0.164	1.000	1.000	1.000
50	0.000	0.000	0.327	0.000	0.000	0.164	1.000	1.000	1.000
51	0.164	0.000	0.000	0.082	0.000	0.000	1.000	1.000	1.000
52	0.327	0.000	0.000	0.164	0.000	0.000	1.006	1.005	1.010
53	0.327	0.000	0.000	0.164	0.000	0.000	1.010	1.009	1.014
54	0.000	0.000	0.000	0.000	0.000	0.000	1.012	1.012	1.017
55	0.164	0.000	0.000	0.082	0.000	0.000	1.012	1.012	1.017
56	0.000	0.164	0.000	0.000	0.082	0.000	1.012	1.012	1.017
57	0.000	0.000	0.000	0.000	0.000	0.000	1.020	1.017	1.023
58	0.000	0.164	0.000	0.000	0.082	0.000	0.000	1.017	0.000
59	0.000	0.164	0.000	0.000	0.082	0.000	0.000	1.017	0.000
60	0.164	0.000	0.000	0.082	0.000	0.000	1.036	1.030	1.038
61	0.000	0.000	0.000	0.000	0.000	0.000	1.036	1.030	1.038
62	0.000	0.000	0.327	0.000	0.000	0.164	1.035	1.029	1.036
63	0.327	0.000	0.000	0.164	0.000	0.000	1.035	1.029	1.035
64	0.000	0.614	0.000	0.000	0.286	0.000	1.034	1.027	1.034
65	0.286	0.286	0.573	0.205	0.205	0.409	1.034	1.027	1.032
66	0.000	0.000	0.614	0.000	0.000	0.286	1.034	1.027	1.031
67	0.000	0.000	0.000	0.000	0.000	0.000	0.993	0.993	0.993

68	0.164	0.000	0.000	0.082	0.000	0.000	0.994	0.000	0.000
69	0.327	0.000	0.000	0.164	0.000	0.000	0.997	0.000	0.000
70	0.164	0.000	0.000	0.082	0.000	0.000	1.000	0.000	0.000
71	0.327	0.000	0.000	0.164	0.000	0.000	1.000	0.000	0.000
72	0.000	0.000	0.000	0.000	0.000	0.000	0.995	0.995	0.996
73	0.000	0.000	0.327	0.000	0.000	0.164	0.000	0.000	0.997
74	0.000	0.000	0.327	0.000	0.000	0.164	0.000	0.000	1.000
75	0.000	0.000	0.327	0.000	0.000	0.164	0.000	0.000	1.000
76	0.859	0.573	0.573	0.654	0.409	0.409	0.997	0.997	0.997
77	0.000	0.327	0.000	0.000	0.164	0.000	0.999	0.999	0.999
78	0.000	0.000	0.000	0.000	0.000	0.000	1.000	1.000	1.000
79	0.327	0.000	0.000	0.164	0.000	0.000	1.000	1.000	1.000
80	0.000	0.327	0.000	0.000	0.164	0.000	1.000	1.000	1.000
81	0.000	0.000	0.000	0.000	0.000	0.000	1.000	1.000	1.000
82	0.327	0.000	0.000	0.164	0.000	0.000	1.000	1.000	1.000
83	0.000	0.000	0.164	0.000	0.000	0.082	1.000	1.000	1.000
84	0.000	0.000	0.164	0.000	0.000	0.082	0.000	0.000	1.000
85	0.000	0.000	0.327	0.000	0.000	0.164	0.000	0.000	1.000
86	0.000	0.164	0.000	0.000	0.082	0.000	1.000	0.998	0.999
87	0.000	0.327	0.000	0.000	0.164	0.000	1.000	1.000	1.000
88	0.327	0.000	0.000	0.164	0.000	0.000	1.000	0.000	0.000
89	0.000	0.000	0.000	0.000	0.000	0.000	1.000	1.000	1.000
90	0.000	$0.327+0.352^{\#}$	0.000	0.000	0.164	0.000	0.000	0.996	0.000
91	0.000	0.000	0.000	0.000	0.000	0.000	1.000	1.000	1.000
92	0.000	0.000	0.327	0.000	0.000	0.164	0.000	0.000	0.999
93	0.000	0.000	0.000	0.000	0.000	0.000	1.000	1.000	1.000
94	0.327	0.000	0.000	0.164	0.000	0.000	1.000	0.000	0.000
95	0.000	0.164	0.000	0.000	0.082	0.000	1.000	1.000	1.000
96	0.000	0.164	0.000	0.000	0.082	0.000	0.000	1.000	0.000
97	0.000	0.24^{*}	0.000	0.000	0.000	0.000	0.995	0.996	0.996
98	0.327	0.000	0.000	0.164	0.000	0.000	0.997	0.997	0.997
99	0.000	0.327	0.000	0.000	0.164	0.000	1.000	0.999	0.999
100	0.000	0.000	0.327	0.000	0.000	0.164	1.000	1.000	1.000
101	0.000	0.000	0.000	0.000	0.000	0.000	0.997	0.998	0.999
102	0.000	0.000	0.164	0.000	0.000	0.082	0.000	0.000	1.000
103	0.000	0.000	0.327	0.000	0.000	0.164	0.000	0.000	1.000
104	0.000	0.000	0.327	0.000	0.000	0.164	0.000	0.000	1.000
105	0.000	0.000	0.000	0.000	0.000	0.000	0.998	0.999	1.000

106	0.000	0.327	0.000	0.000	0.164	0.000	0.000	1.000	0.000
107	0.000	0.327+0.584#	0.000	0.000	0.164	0.000	0.000	1.000	0.000
108	0.000	0.000	0.000	0.000	0.000	0.000	1.000	1.000	1.000
109	0.327	0.000	0.000	0.164	0.000	0.000	1.000	0.000	0.000
110	0.000	0.000	0.000	0.000	0.000	0.000	1.000	0.000	0.000
111	0.164	0.000	0.000	0.082	0.000	0.000	1.000	0.000	0.000
112	0.164	0.000	0.000	0.082	0.000	0.000	1.000	0.000	0.000
113	0.327	0.000	0.000	0.164	0.000	0.000	1.000	0.000	0.000
114	0.164	0.000	0.000	0.082	0.000	0.000	1.000	0.000	0.000
115	0.000	0.000	0.000	0.000	0.000	0.000	1.000	1.000	1.000
135	0.000	0.000	0.000	0.000	0.000	0.000	0.988	0.950	0.950
149	0.000	0.000	0.000	0.000	0.000	0.000	1.000	1.000	1.000
150	0.000	0.000	0.000	0.000	0.000	0.000	1.000	1.000	1.000
151	0.000	0.000	0.000	0.000	0.000	0.000	0.999	0.997	1.001
152	0.000	0.000	0.000	0.000	0.000	0.000	1.036	1.030	1.038
160	0.000	0.000	0.000	0.000	0.000	0.000	0.995	0.996	0.996
197	0.000	0.000	0.000	0.000	0.000	0.000	1.000	1.000	1.000
250	0.000	0.000	0.000	0.000	0.000	0.000	1.000	1.000	1.000
300	0.000	0.000	0.000	0.000	0.000	0.000	1.000	1.000	1.000
450	0.000	0.000	0.000	0.000	0.000	0.000	1.036	1.030	1.038

The DU and MGOs offered prices for IEEE 123-bus system are shown in the Figure 5.17. The profits of all MGs are reduced in the IEEE 123-bus system as compared to the IEEE 33-bus and the 25-bus unbalanced distribution system. The power exchange price of MGOs with DU depends on the base price offered by DU and demand of all MGOs. The number of MGOs considered in the IEEE 123-bus system case is five, while the number of MGOs considered in the IEEE 33-bus and the 25-bus unbalanced distribution system is three. Therefore, in the IEEE 123-bus unbalanced distribution system the

Table 5.9: *Case II* outcomes for IEEE 123-bus unbalanced distribution system

	MG1	MG2	MG3	MG4	MG5	DU
$\sum_n F^n_{EUA}$	718.747	1234.006	769.619	685.772	771.673	-
F^m_{MGO}	6784.665	7476.367	6234.061	7512.678	6752.520	-
F^C_{DU}	-	-	-	-	-	1408.5519

power exchange price is increased and thus the profits of MGOs are decreased. Figure 5.16 shows the voltage level of three phases of the IEEE 123-bus unbalanced distribution system. The white space in the heat maps indicates the unavailability of the phase line to the corresponding BUS indicated at Y-axis. As compared to IEEE 33-bus and 25-bus distribution systems, the voltage level is approximately 1.0 p.u. or greater than 1.0 p.u. most of the time interval.

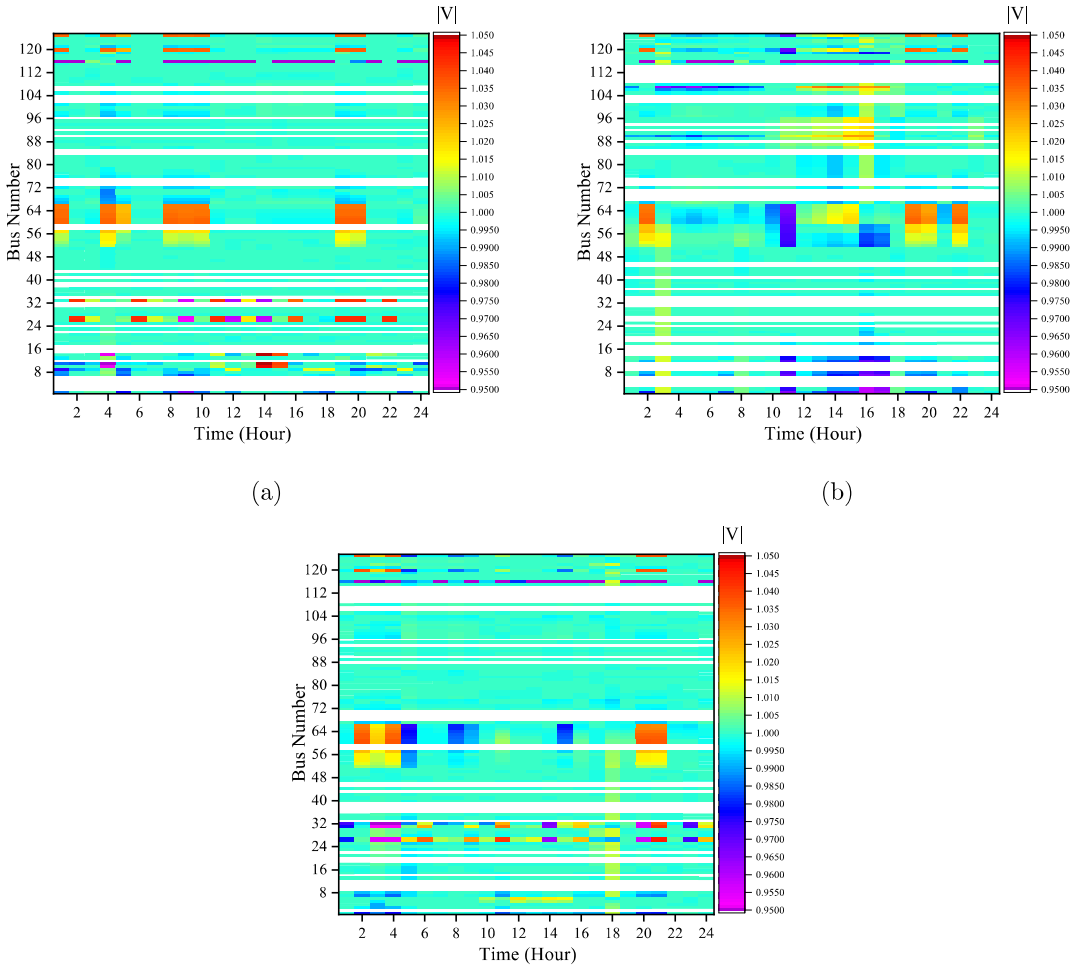

Figure 5.16: Voltage level of IEEE 123-bus system (a) Phase-A, (b) Phase-B, (c) Phase-C. (White space in the heat maps indicates the unavailability of the phase line to the corresponding BUS indicated at Y-axis)

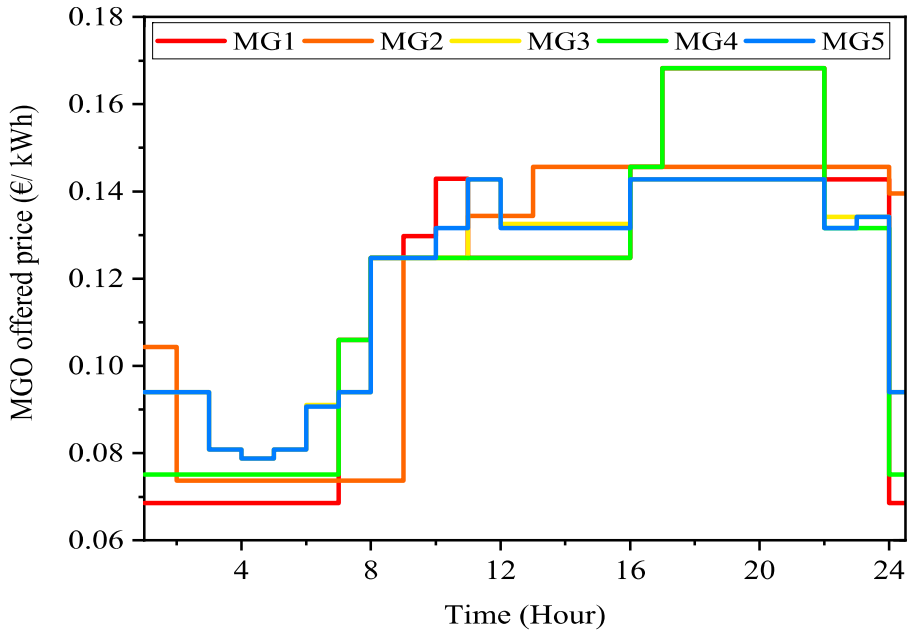

(a)

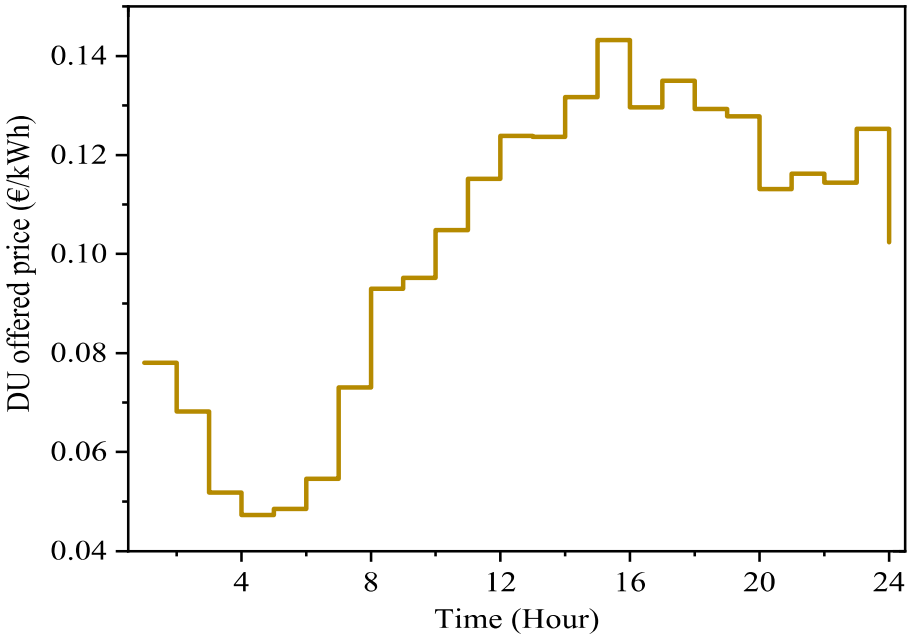

(b)

Figure 5.17: Offered prices for IEEE 123-bus system (a) MGOs' offered price to EUAs, (b) Base price offered by DU

5.6 Summary

The numerical results establish the effectiveness of the proposed energy management framework in realizing the objectives of multiple decision-making agents—DU, MGOs, and EUAs. The proposed participation strategy leads to an increase in the profits of MGOs, decrease in the cost of DU, and reduced peak demand maintaining the similar average price as in the case of non-interactive approach. The minimum voltage level and load profile are improved with the interaction of all the resources of the DU, MGOs, and EUAs. The net power exchange of MGO with DU decreases as the import power decreases and export power increases. Similarly, electricity imports by DU from the main grid also reduce. The results show that the energy cost for DU increases as the level of tolerable uncertainty in risk-averse decision-making increases, whereas the energy cost for DU decreases with the level of uncertainty required in the risk-seeking decision-making of MGO.